Cavitandi

ciclotriveratrilene

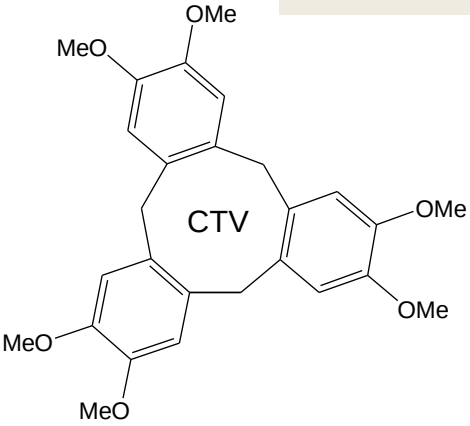

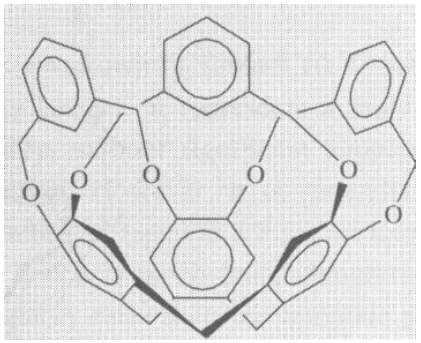

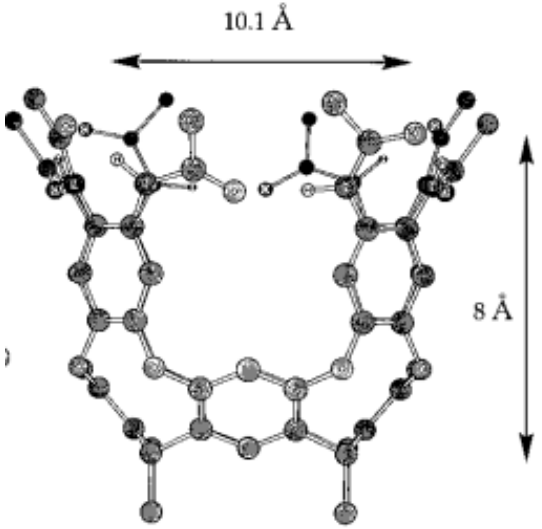

Cucurbiturili

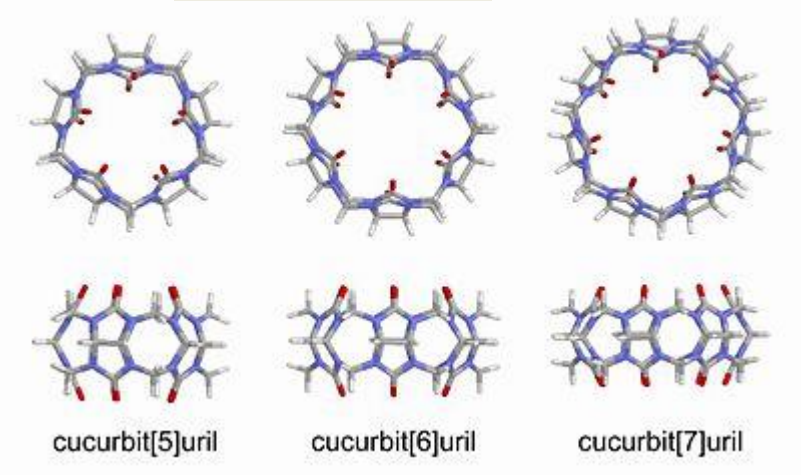

Ciclodestrine

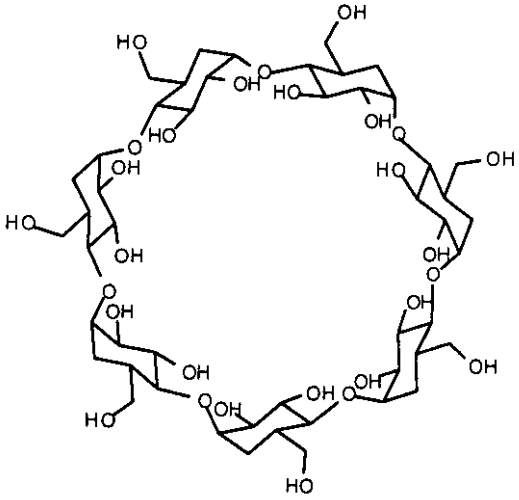

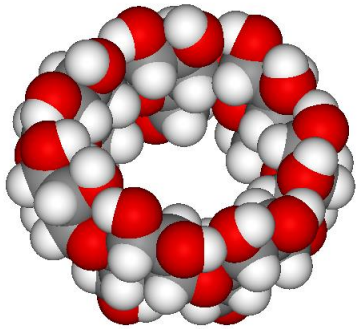

Capsule Molecolari

Unione di due cavitandi

Connessione covalente
Legame idrogeno
Legame di coordinazione

Pre-organizzazione

Protezione dal solvente esterno
Rallentamento delle cinetiche di scambio
Stabilizzazione di specie reattive
Reazioni catalitiche
Drug delivery

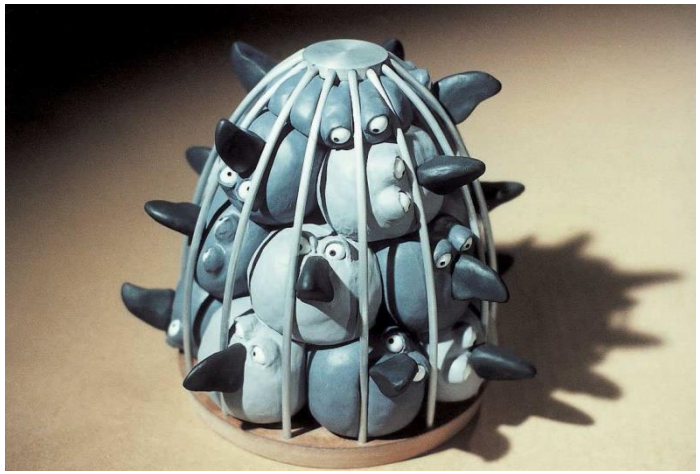

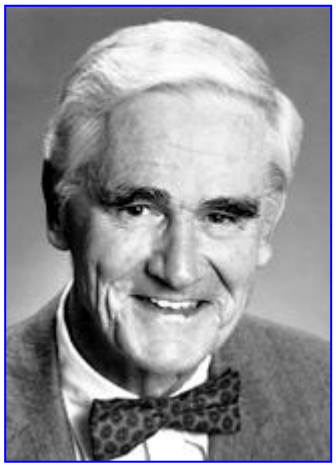

Carcerando:

Contenitore molecolare chiuso (capsula) che definisce cavità sferica, i guest sono intrappolati (all'atto della sintesi) entrata e uscita solo per rottura di legame covalente, i.e. velocità di scambio virtualmente nulla

Carcerandi

Benzil-tiolo

benzil cloruro
(o bromuro)

Alta dliuz

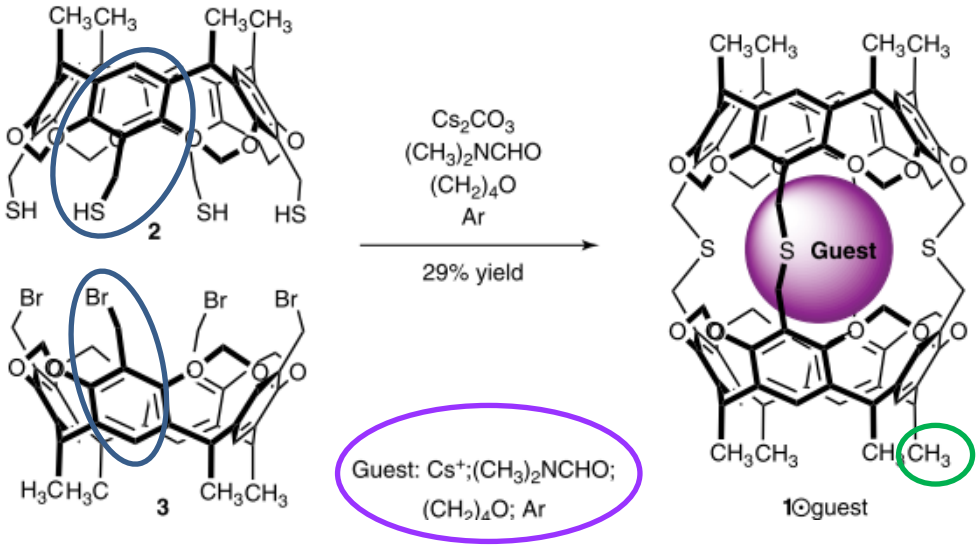

Insolubilità = caratterizz via IR, FAB-MS, analisi elementare, test chimici
FAB-MS dei carciplessi

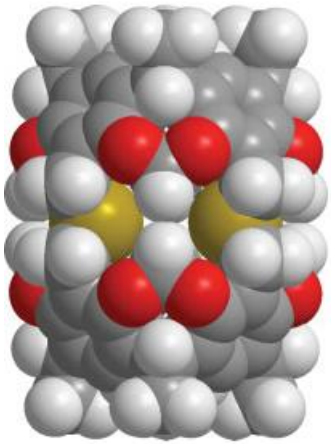

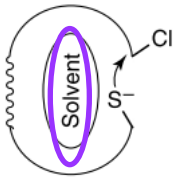

Carcerandi

fenolo

bromo-clorometano

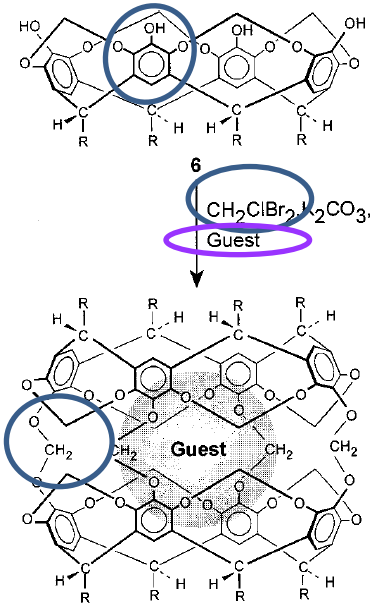

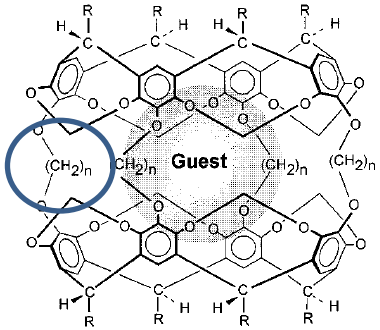

11•Guest n = 2 R = CH_2CH_2Ph
12•Guest n = 3 or $C_{11}H_{23}$

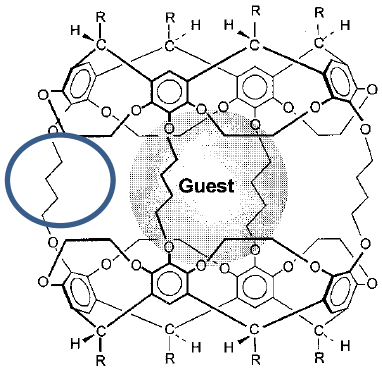

13•Guest R = $(CH_2)_4CH_3$

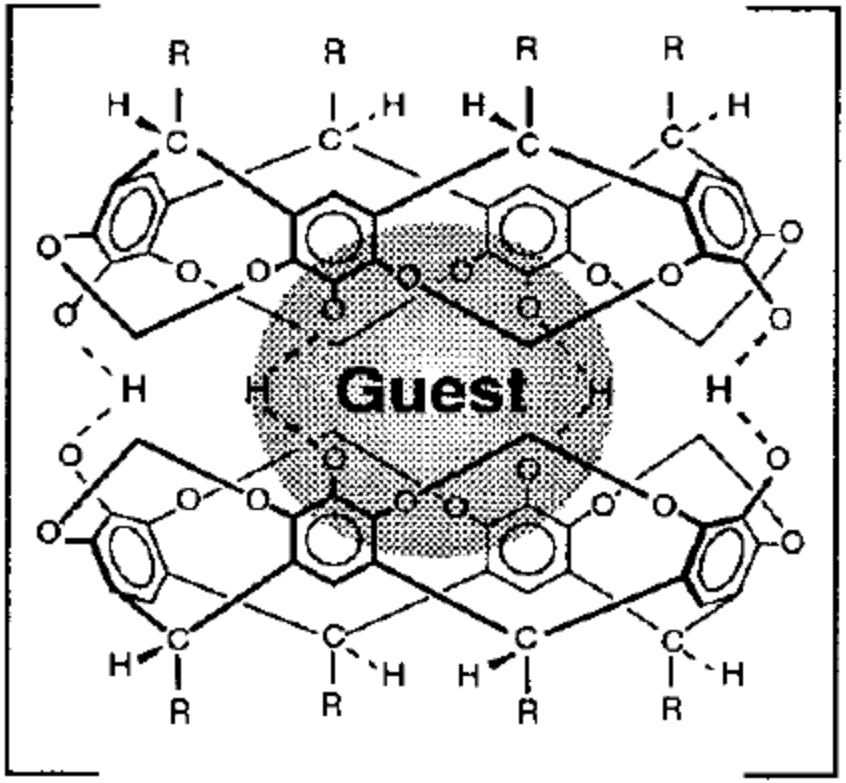

Complex **3**•Guest

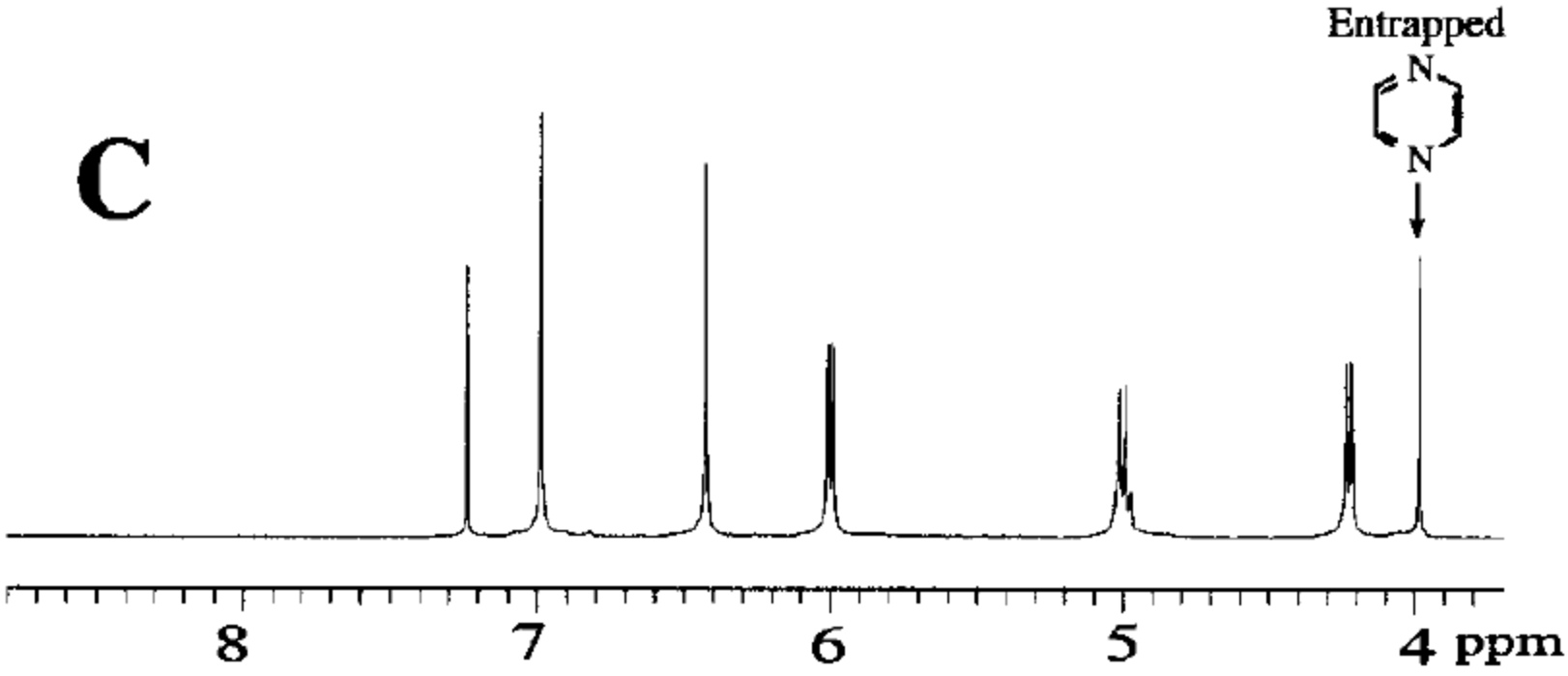
C
Entrapped
N
N
8
7
6
5
4 ppm

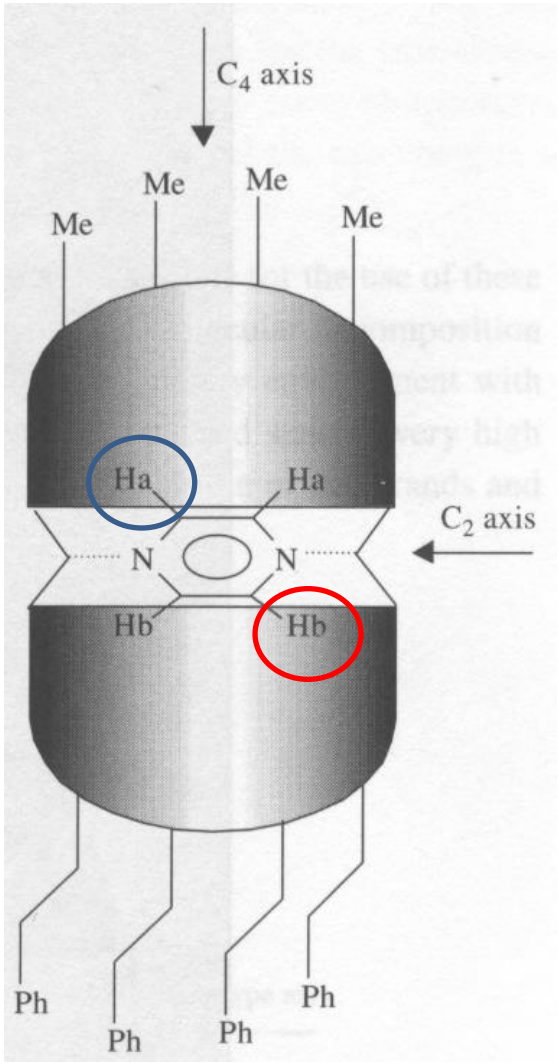
C4 axis
Me
Me
Me
Me
Ha
Ha
C2 axis
N
N
Hb
Hb
Ph
Ph
Ph
Ph

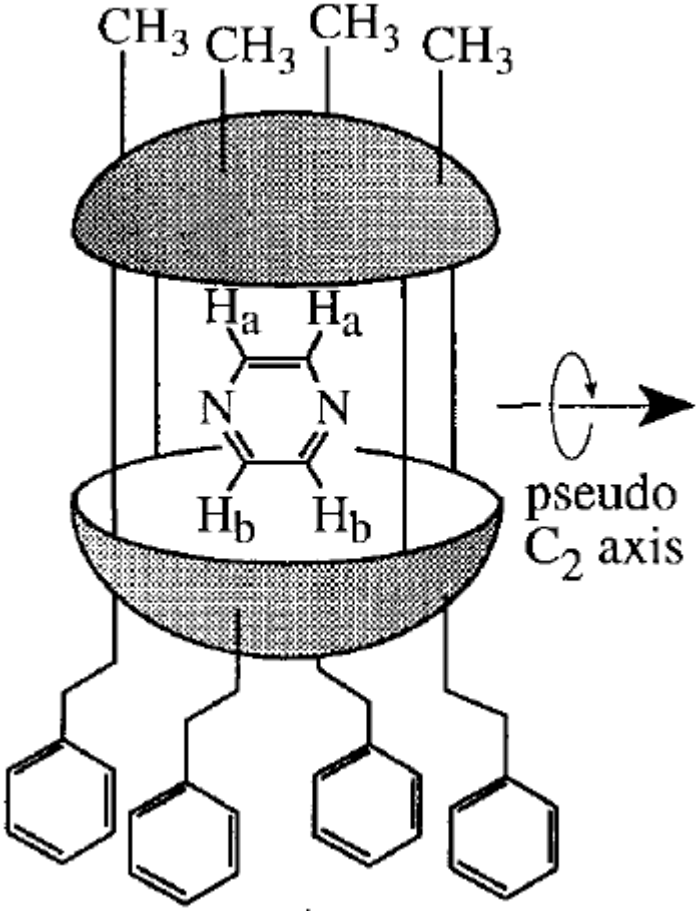
CH3 CH3 CH3 CH3
Ha Ha
N N
Hb Hb
pseudo
C2 axis

tively. The signals for pyrazine in asymmetric complex **3c**•pyrazine consisted of two *meta*-split doublets at 4.31 ($J = 1$ Hz) and 4.35 ppm ($J = 1$ Hz).[16] This confirms that pyrazine is oriented in complex **3b**•pyrazine with its nitrogens at the equator and its hydrogens extending into the bowls (structure **A**, Figure 3). The activation energy for rotation of pyrazine about the pseudo-C_2 axes in asymmetric complex **3c**•pyrazine was measured by variable-temperature ^{1}H NMR spectroscopy to be 18 kcal/ mol,[17] which agrees well with the 19 kcal/mol activation

(17) The activation barrier for rotation of pyrazine about the pseudo-C_2 axes of asymmetric complex **3c**•pyrazine was calculated to be 18.3 kcal/ mol based on a coalescence temperature (T_c) of 353 K and separation of the signals ($\Delta\delta_{Hz}$) of 14.3 Hz using the following equation: $\Delta G_c^{\ddagger} = RT_c$-$[22.96 + \ln(T_c/\Delta\delta_{Hz})]$ where $\Delta G_c^{\ddagger}$ is the activation barrier in kcal/mol; T_c is the temperature of coalescence, and $\Delta\delta_{Hz}$ is the separation of the signals in Hz. See: Abraham, R. J.; Fisher, J.; Loftus, P. *Introduction to NMR Spectroscopy*; Wiley: New York, 1990; pp 194−197.

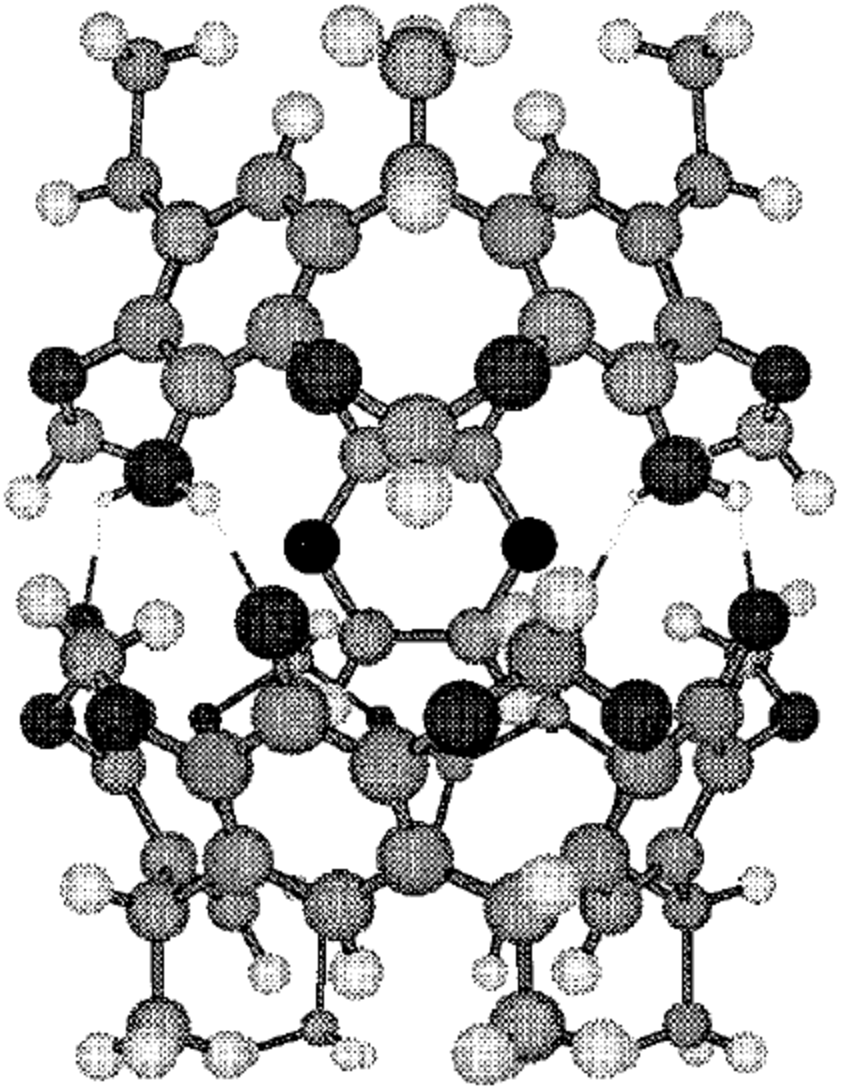

Emicarcerando:

Contenitore molecolare chiuso (capsula) che definisce cavità sferica, i guest sono intrappolati (all'atto della sintesi) - entrata e uscita senza rottura di legame covalente, i.e. velocità di scambio misurabile

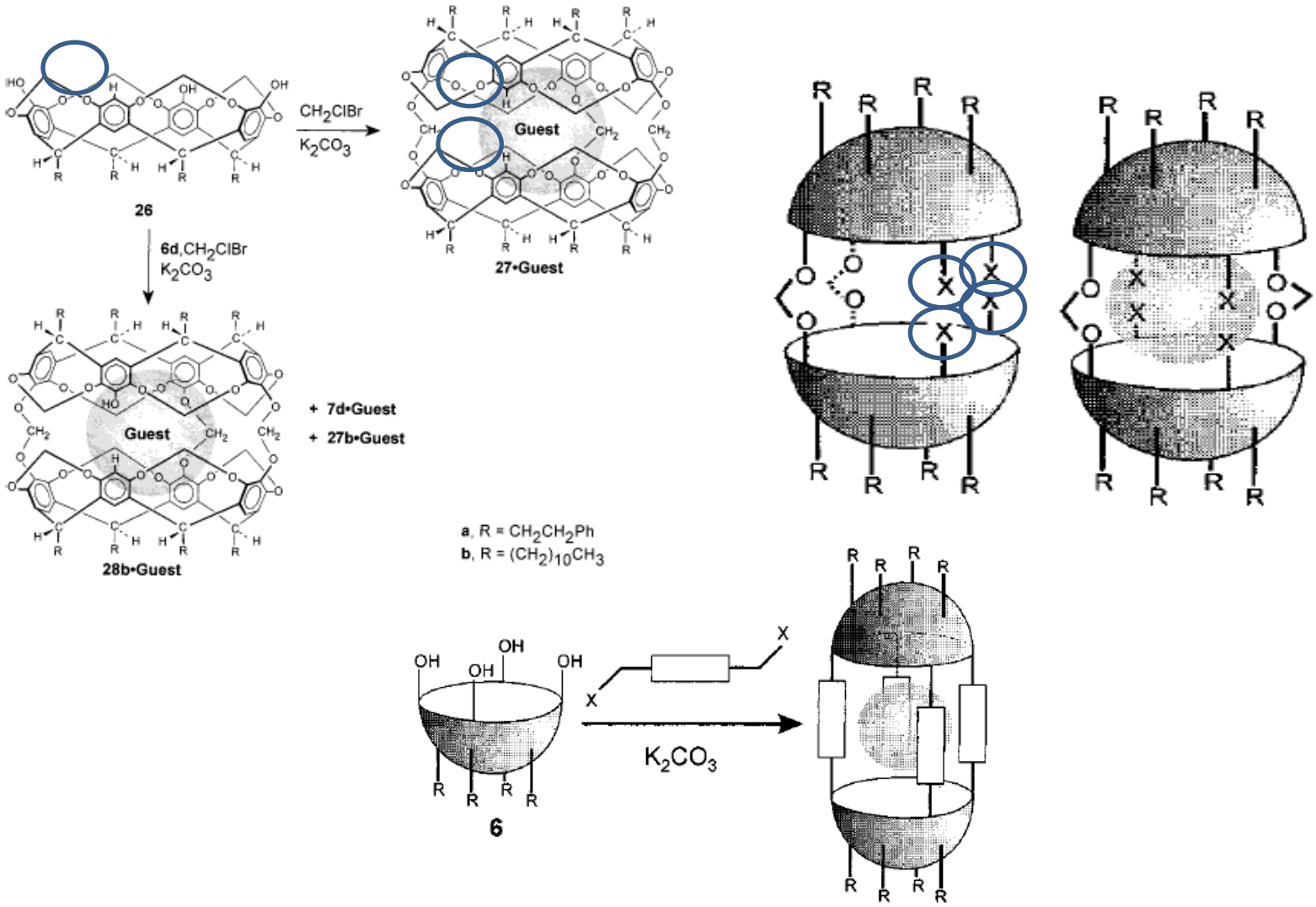

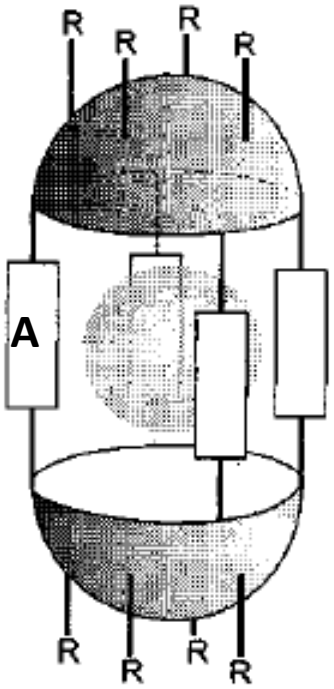

A
$O–CH_2–O$
$S–CH_2–S$
$O–(CH_2)_4–O$
$O–(CH_2)_5–O$
$O–(CH_2)_6–O$
$O–(CH_2)_2O(CH_2)_2–O$


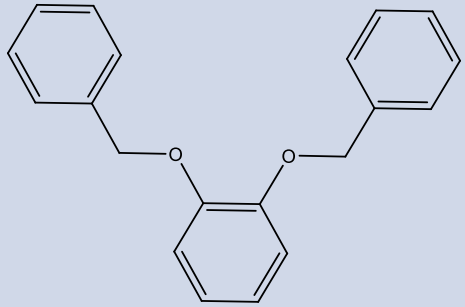

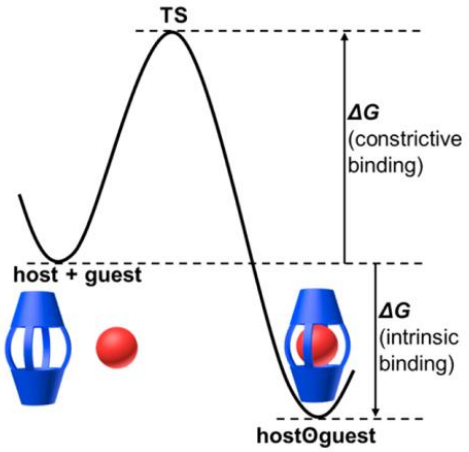

guests. In host−guest systems, there are two energetic quantities associated with guest binding—constrictive and intrinsic binding. The constrictive binding[11,12] is the activation energy required for a guest to enter the host, while intrinsic binding is the change in energy upon formation of the host−guest complex from free host and guest. Intrinsic binding energy determines the equilibrium constant for binding; the intrinsic binding energy plus the constrictive binding energy determines the kinetic barrier to decomplexation.[12]

Intrinisic binding, the free energy of complexation, depends on the magnitude of the noncovalent interactions between the guest and the host's inner surface.

Constrictive binding, activation energy required for a guest to enter OR exit the inner cavity of a hemicarcerand through a size restricting portal in the host's skin.

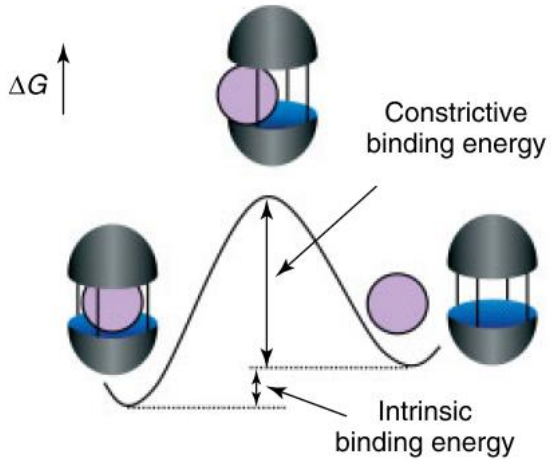

Constrictive binding: aumenta con le dimensioni del guest, diminuisce con le dimensioni dei portali, e con l'aumento della flessibilità dei linker (T).

Gating: Gating in host-guest chemistry refers to conformational changes that occur in response to some stimulus, resulting in opening or closing of a physical barrier that controls access to the host.

- **Thermal Gating**
- **Stimulated Gating**

Gate mechanisms (molecular mechanics calculations) – **French door**
chair-to-boat transition of the methylene bridges, calculated barrier 22 kcal/mol.

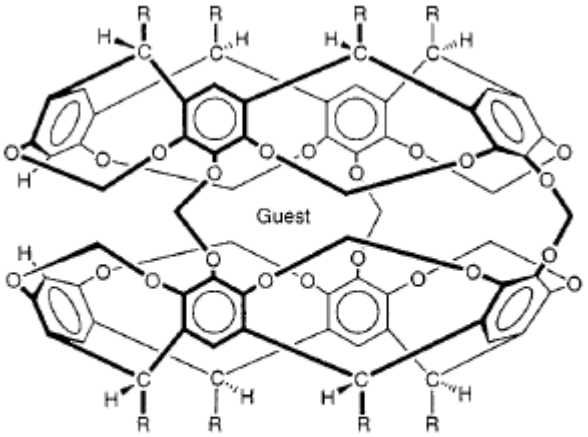

12⊙ Guest

R = CH_2CH_2Ph

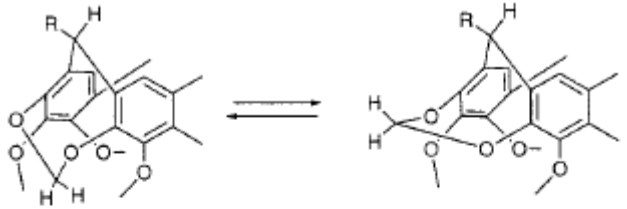

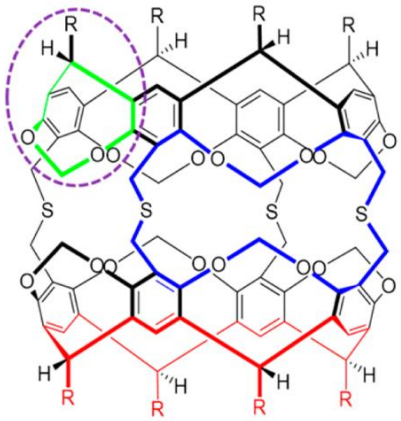

1a. R = $(CH_2)_2Ph$
1b. R = Me

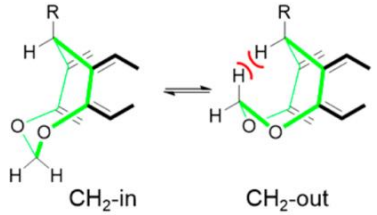

Gate mechanisms (molecular mechanics calculations) – **Sliding door**
twisting and untwisting of the two host cavitands – measured barrier (VT NMR) 12.6 kcal/mol

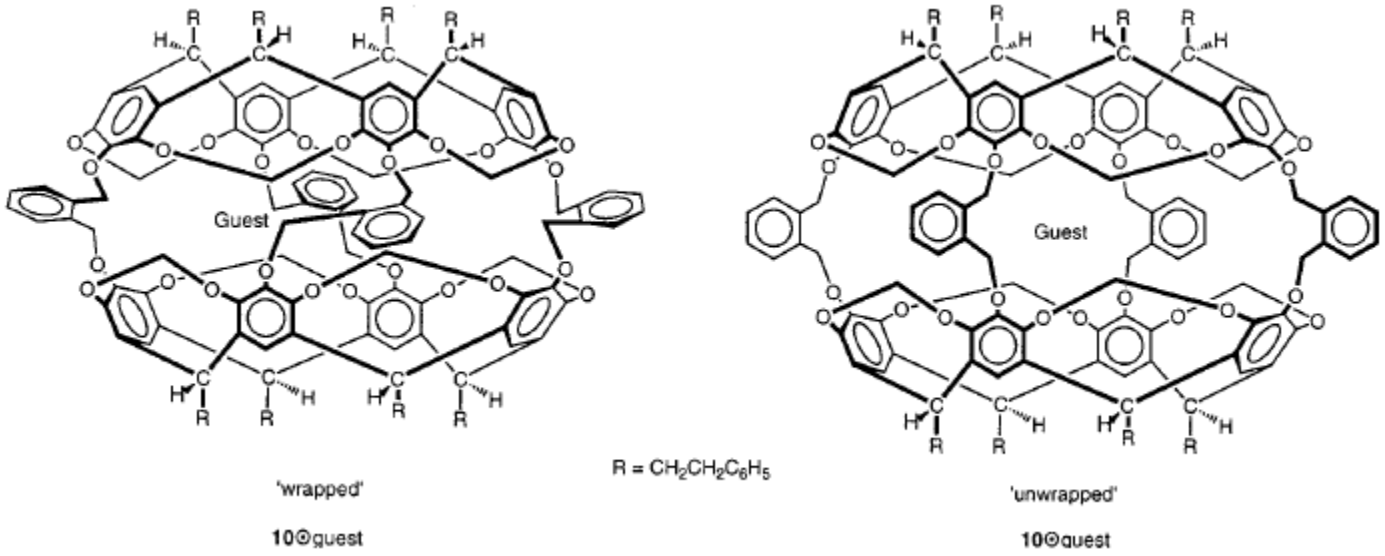

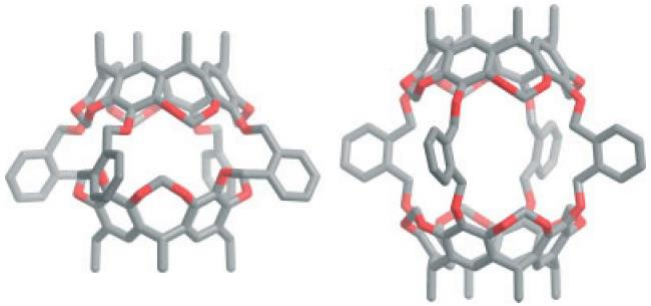

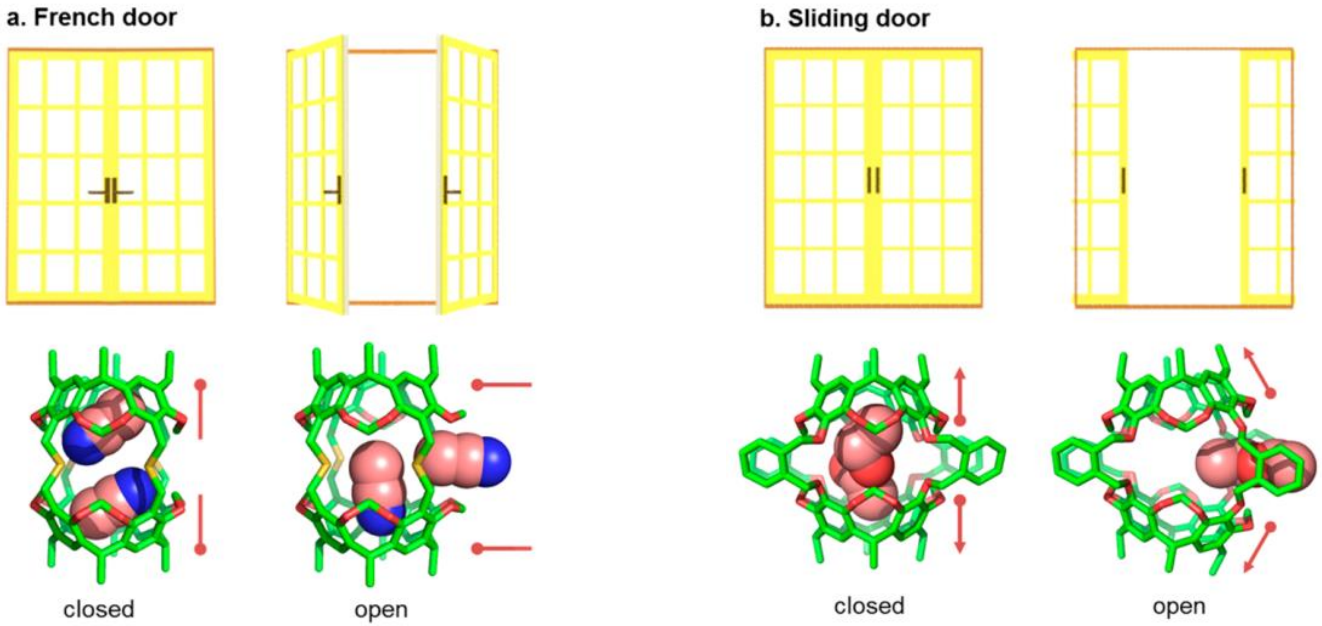
a. French door
b. Sliding door
closed
open
closed
open

Stimulated Gating

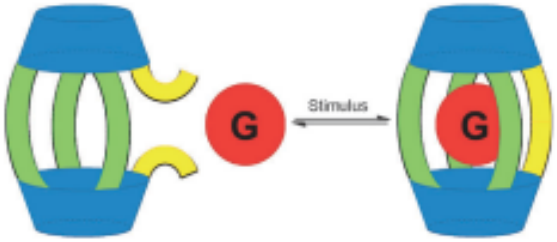

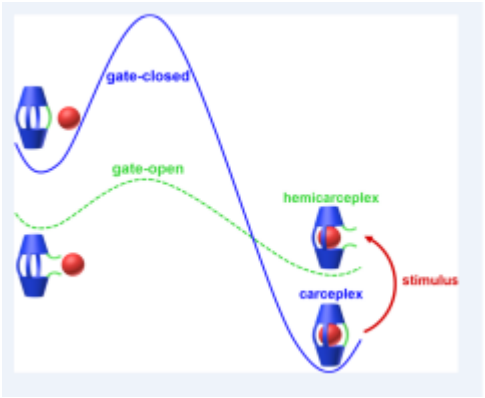

Redox Gating

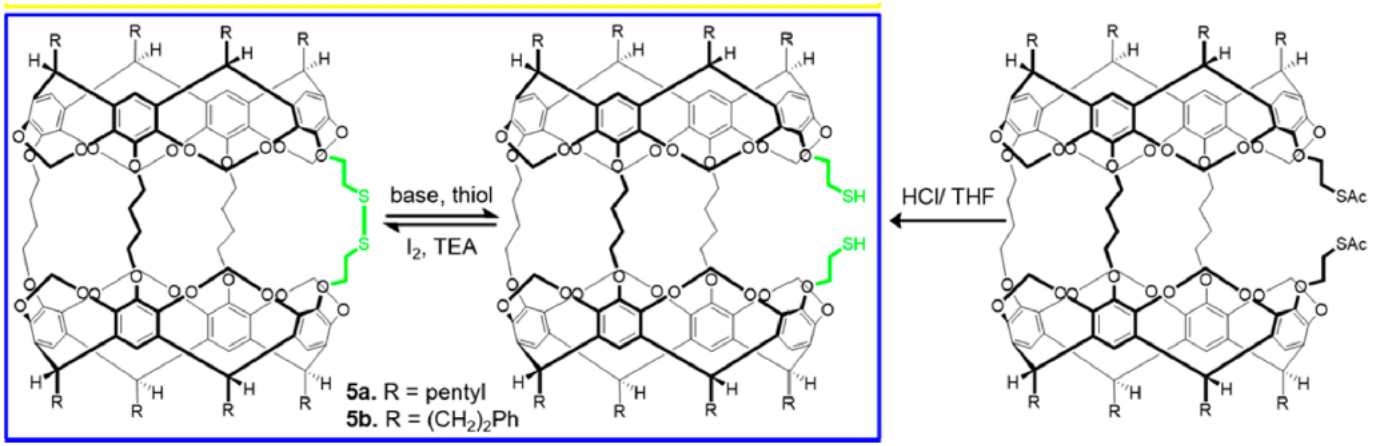

Photochemical Gating

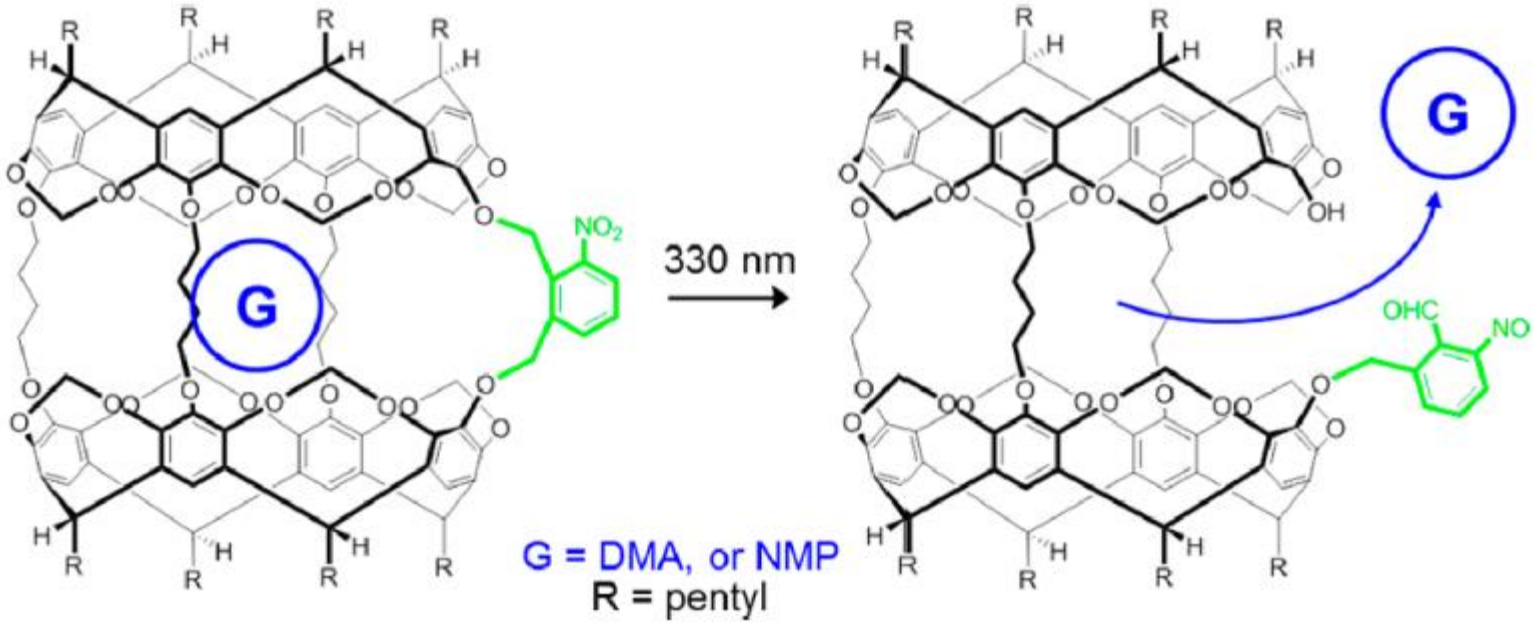

Host–Guest Chemistry

DOI: 10.1002/anie.201205376

Reversible Photochemically Gated Transformation of a Hemicarcerand to a Carcerand**

*Hao Wang, Fang Liu, Roger C. Helgeson, and Kendall N. Houk**

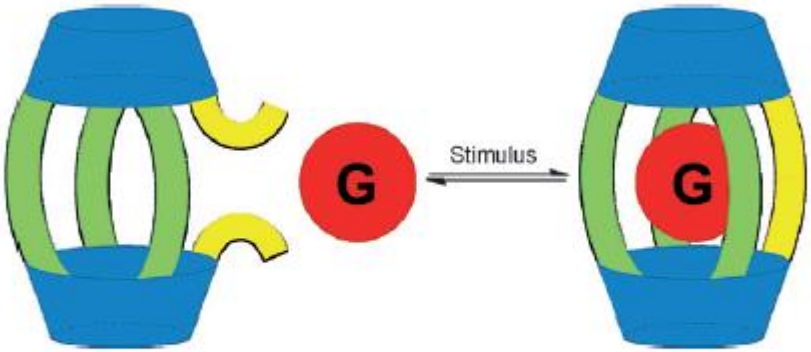

Figure 1. Gating in container molecules converts a hemicarcerand (left) into a carcerand (right).

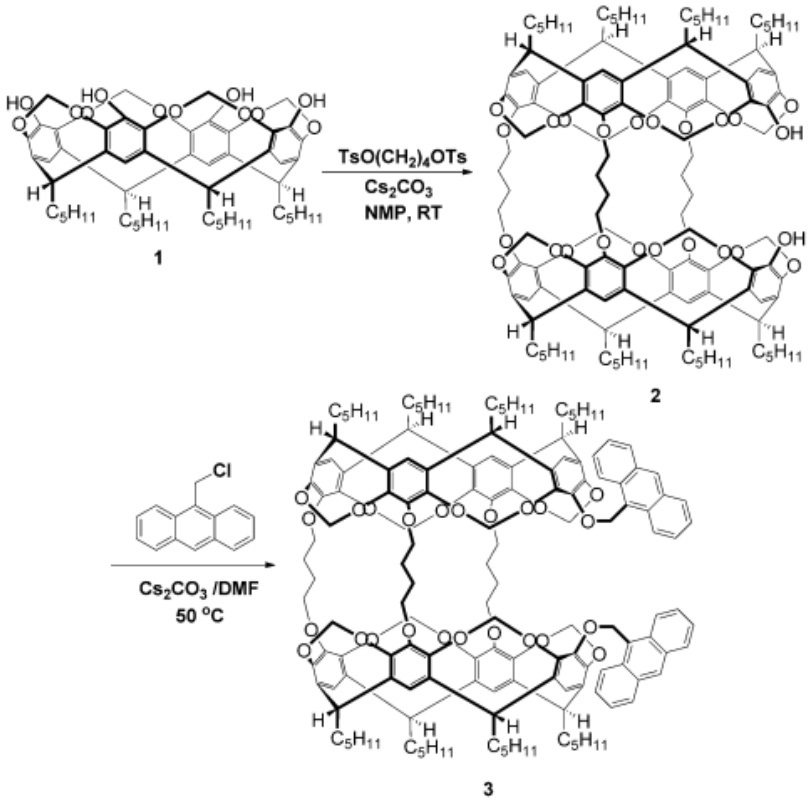

1

2

3

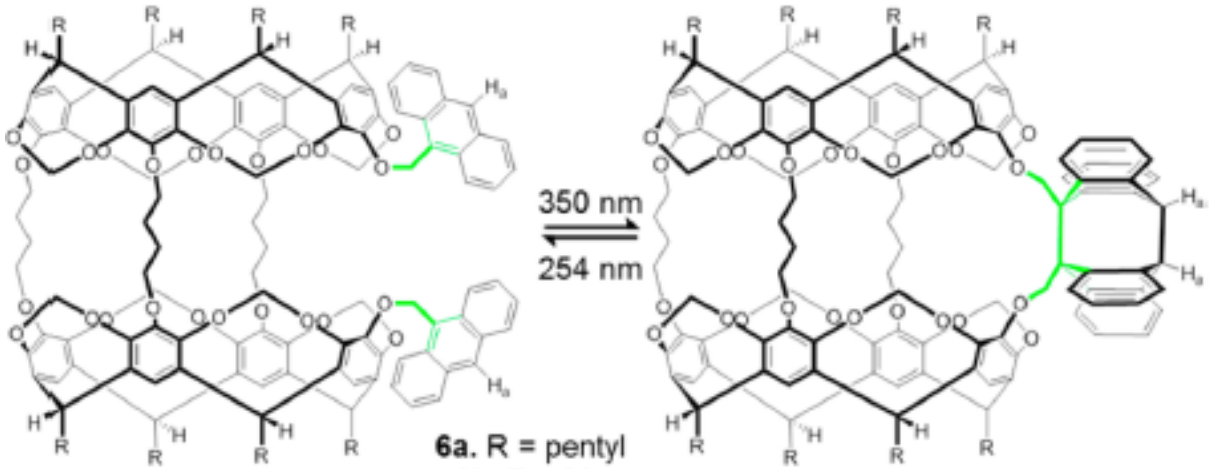

6a. R = pentyl
6b. R = Me

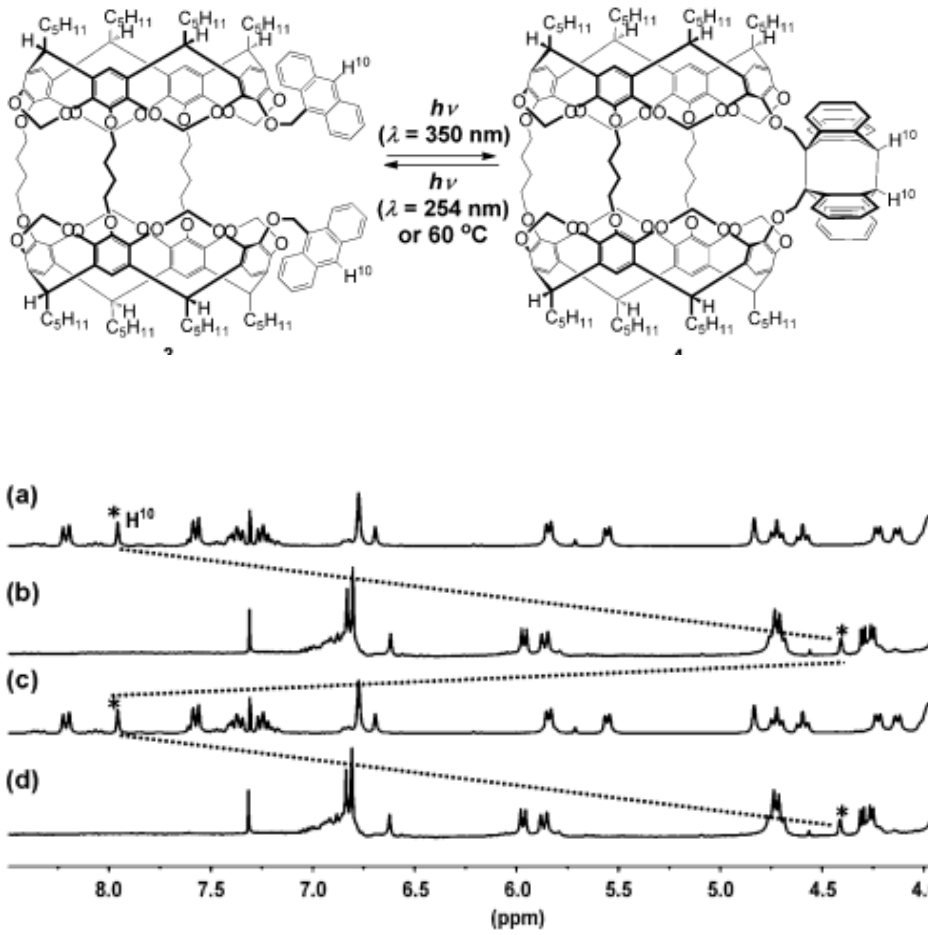

Figure 3. Partial ^{1}H NMR spectra (400 MHz, $CDCl_3$) of a) host **3** b) irradiation of host **3** with light at 350 nm for 1 h, c) irradiation of b with light at 254 nm for 1 h or heating at 60 °C for 20 min, d) irradiation of c with light at 350 nm for 1 h.

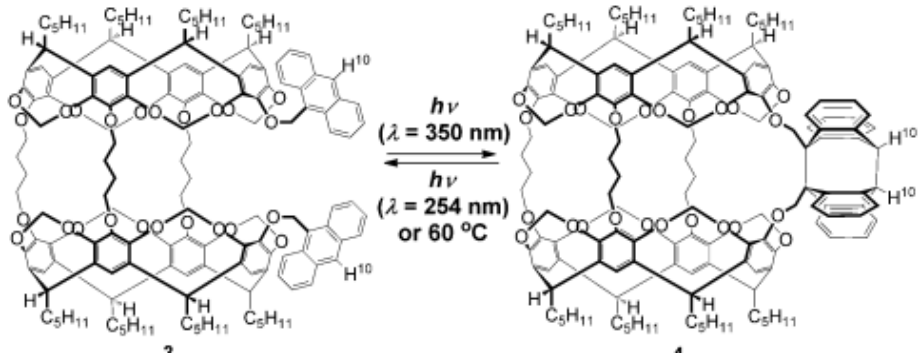
hν
(λ = 350 nm)
hν
(λ = 254 nm)
or 60 °C

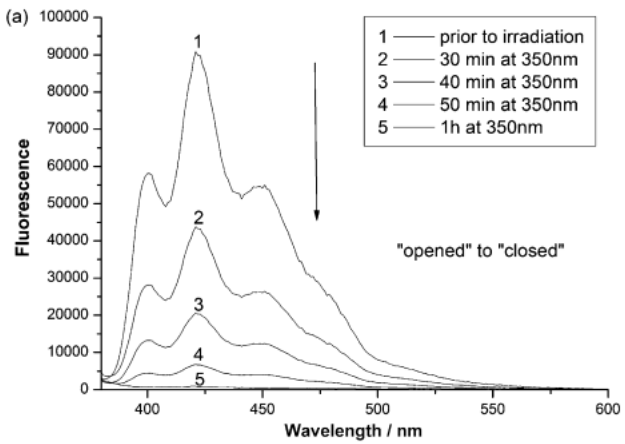
(a)
Fluorescence
Wavelength / nm
1 —— prior to irradiation
2 —— 30 min at 350nm
3 —— 40 min at 350nm
4 —— 50 min at 350nm
5 —— 1h at 350nm
"opened" to "closed"

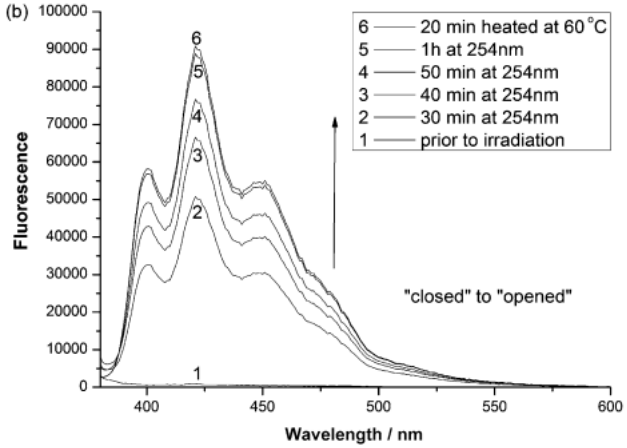
(b)
Fluorescence
Wavelength / nm
6 —— 20 min heated at 60 °C
5 —— 1h at 254nm
4 —— 50 min at 254nm
3 —— 40 min at 254nm
2 —— 30 min at 254nm
1 —— prior to irradiation
"closed" to "opened"

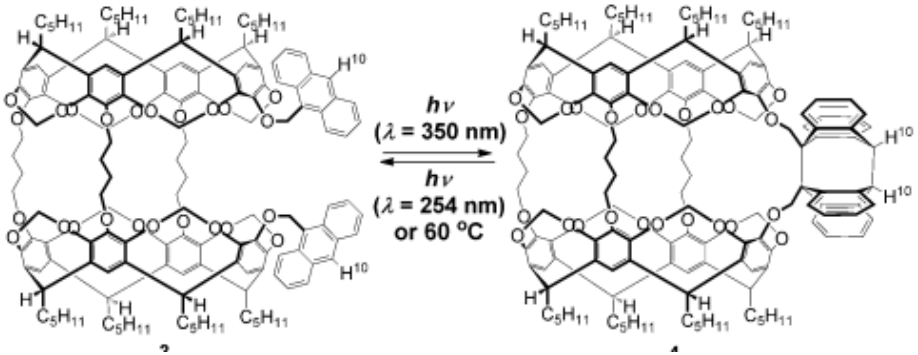
hν
(λ = 350 nm)
hν
(λ = 254 nm)
or 60 °C

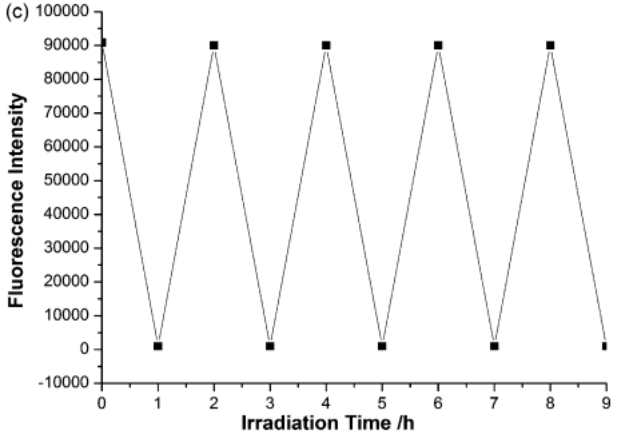
(c)
Fluorescence Intensity
Irradiation Time /h
100000
90000
80000
70000
60000
50000
40000
30000
20000
10000
0
-10000
0
1
2
3
4
5
6
7
8
9

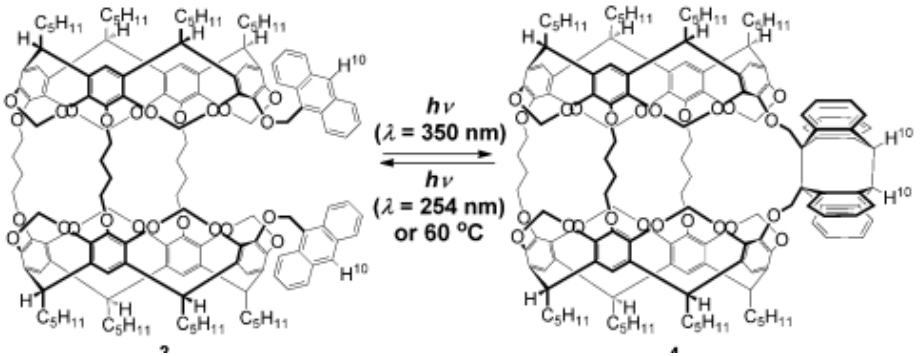

The progress of the photodimerization was also monitored by thin-layer chromatography, which showed only one band after completion of the photodimerization. Photodimer 4 was purified after photolysis at 350 nm. In the high-resolution mass spectrum the molecular ion of photoproduct 4 has the same mass as the parent open-state host 3.

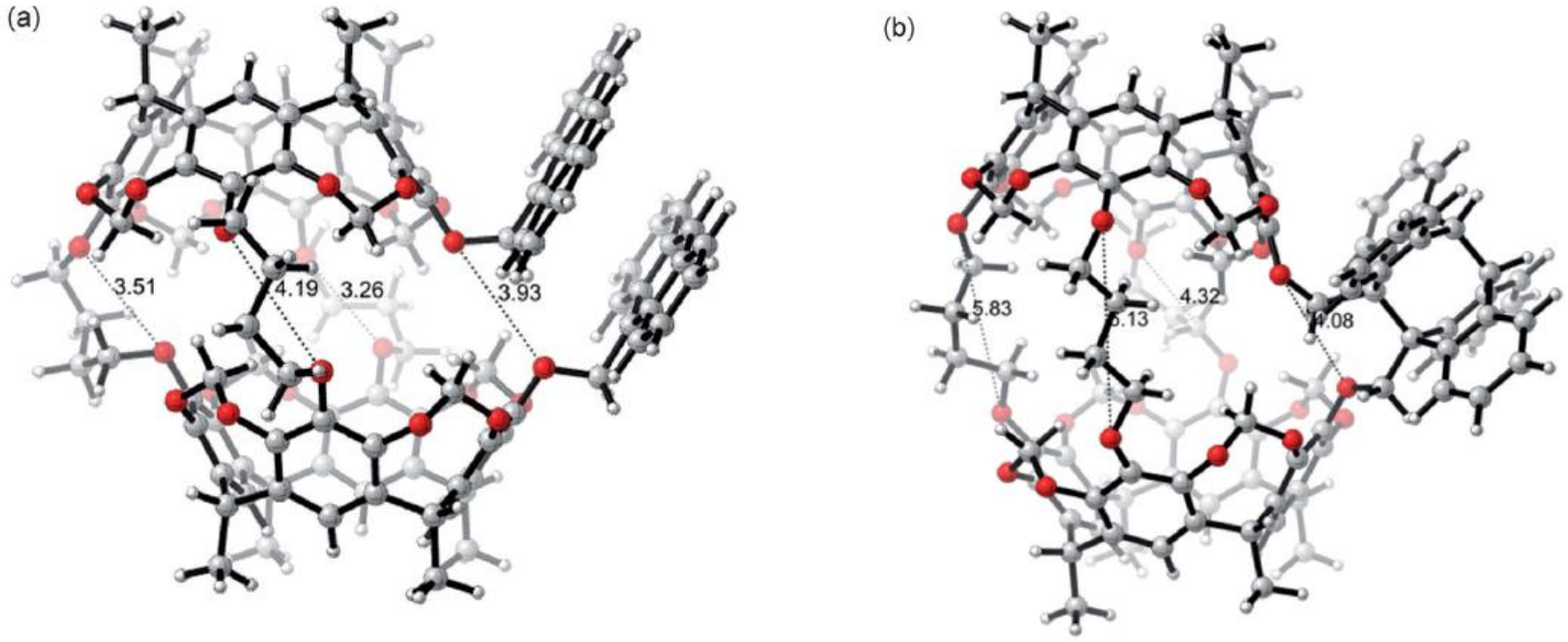
(a)
3.51
4.19
3.26
3.93
(b)
5.83
5.13
4.32
4.08

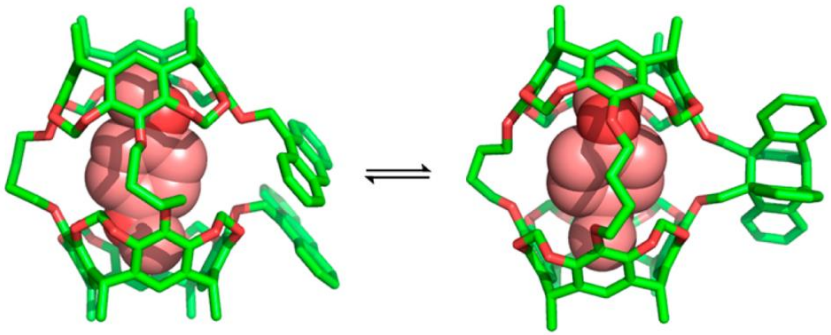

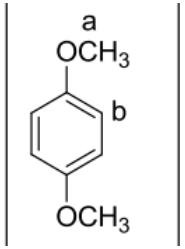

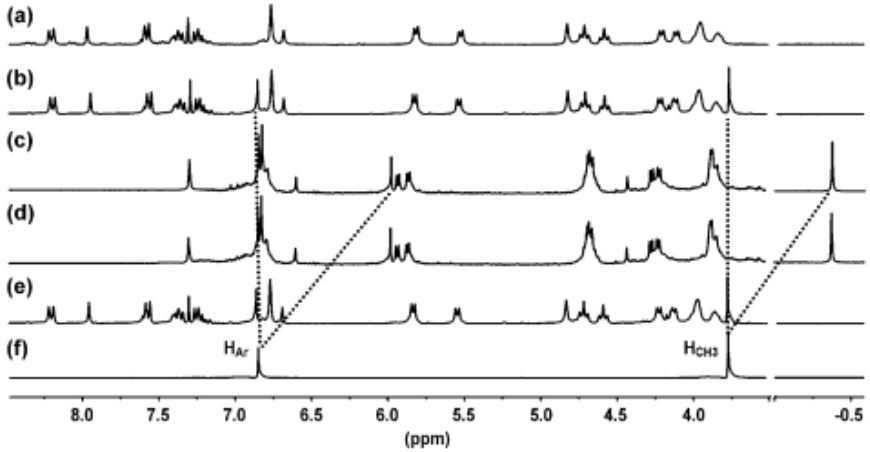

Figure 6. Partial ^{1}H NMR spectra (400 MHz, $CDCl_3$) of a) host **3** b) addition of 1 equiv of 1,4-$(MeO)_2C_6H_4$ into host **3** solution without irradiation, c) **4** ⊙ 1,4-$(MeO)_2C_6H_4$,[16] d) c after 4 weeks in dark and RT, e) irradiation of c with light at 254 nm for 1 h or heating at 60 °C for 20 min, f) guest 1,4-$(MeO)_2C_6H_4$.

(c)

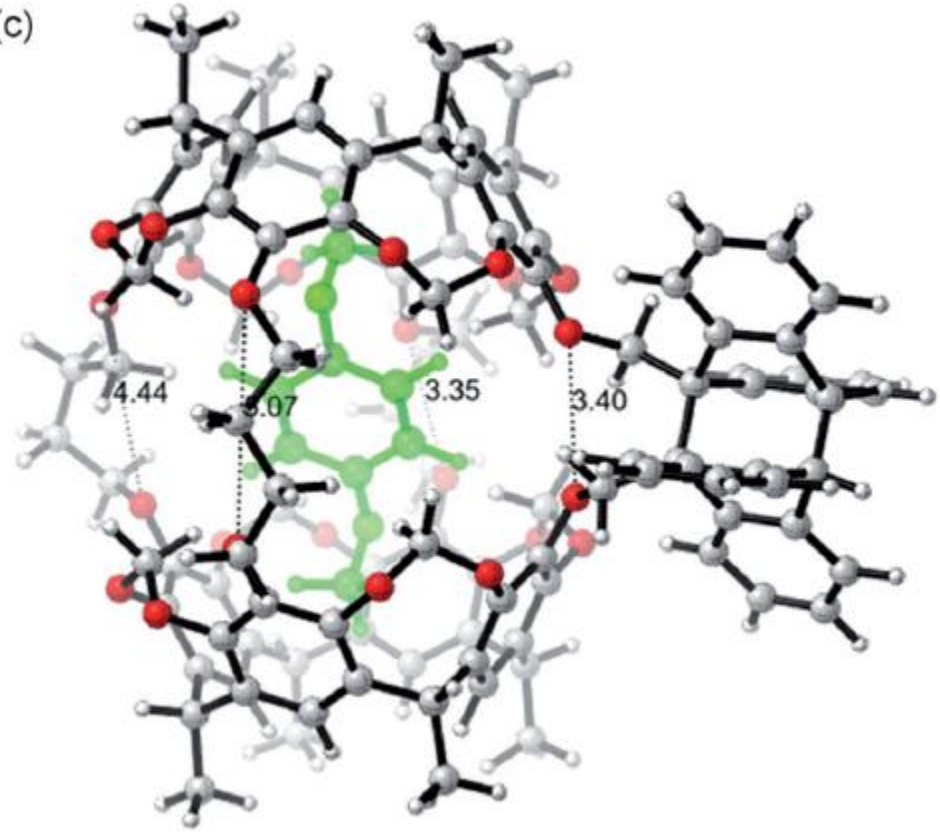

Guest	H	Δδ (ppm)	Guest	H	Δδ (ppm)
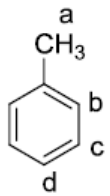	H_a H_b H_c H_d	3.96 1.53 1.85 3.35	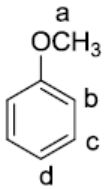	H_a H_b H_c H_d	3.87 1.60 1.95 3.30
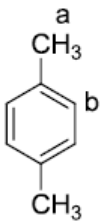	H_a H_b	4.17 1.06	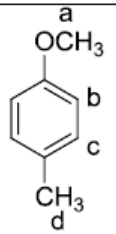	H_a H_b H_c H_d	4.01 0.84 0.98 4.21
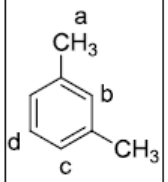	H_a H_b H_c H_d	3.17 hidden 1.86 hidden	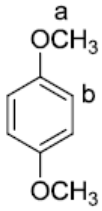	H_a H_b	4.15 0.85
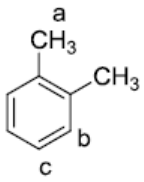	H_a H_b H_c	2.34 1.54 1.95	$CH_aCl_2—CHCl_2$ $CH_aBr_2—CHBr_2$	H_a H_a	0.95 1.02

Table S1: Complexation of **4** with various guest molecules and the chemical shift changes of corresponding Hs (before and after complexations) on the guests.

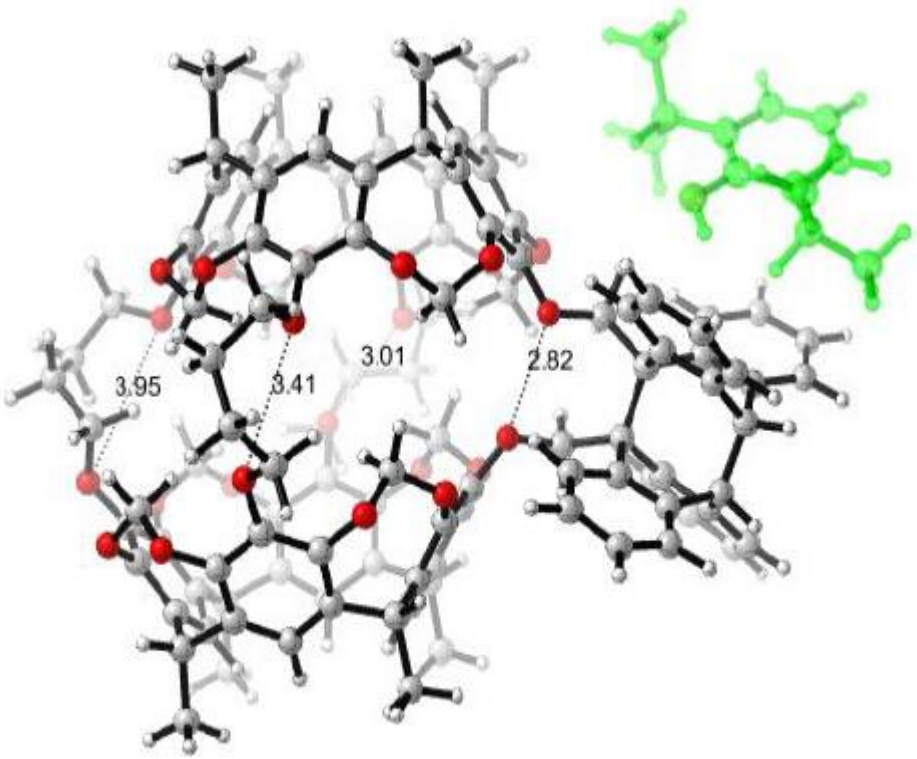

Figure S2: Molecular modelling of complexation of **4** with propofol (2,6-diisopropylphenol) using Schrödinger Macromodel (OPLS_2005, GB/SA $CHCl_3$). (The geometry began with the guest inside the host; the guest came out of the host after the minimization)

In summary, a new reversible photoswitchable gated hemicarcerand containing two anthracene groups was designed and synthesized. The photochemical properties of this system were studied by ^{1}H NMR and fluorescence spectroscopy. The photoswitchable cycle between the open (hemicarcerand) and closed (carcerand) states of the host is well controlled by radiation of different wavelengths, and controlled encapsulation and release of the guest molecules such as 1,4-dimethoxybenzene was observed. We are currently working on enlarging the cavity size of the host as well as increasing the water solubility of the host.

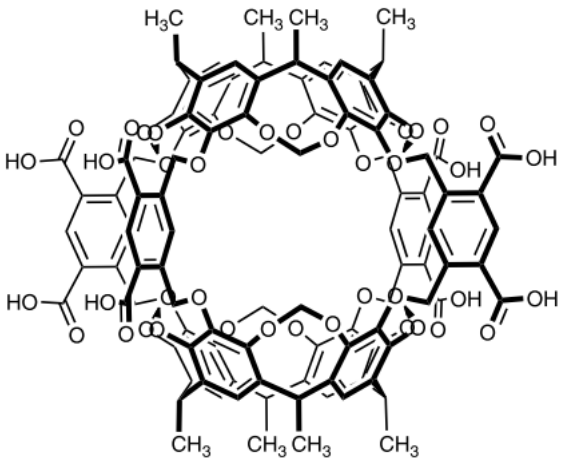

Water soluble octa-acid hemicarcerand:

Hydrophobic effect (higher than cyclodextrines)!

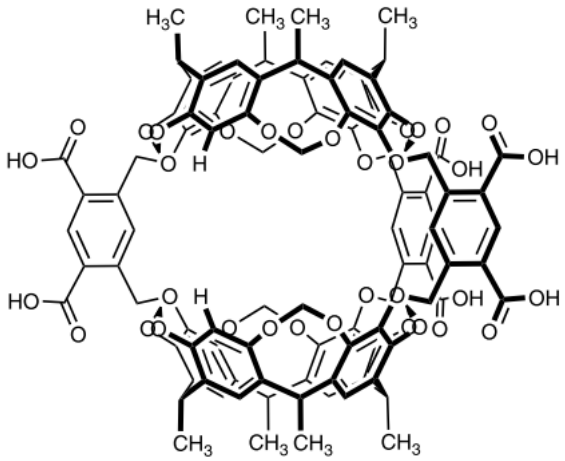

CH-π interactions for isomeric xylenes or dimetoxybenzenes direct the order of affinity:
meta > para >> ortho

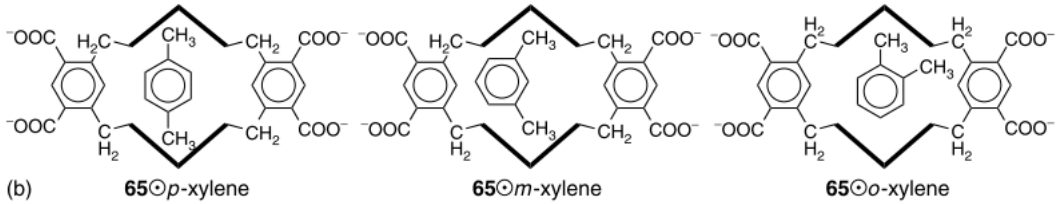

Benzociclobutendione Benzociclopropenone

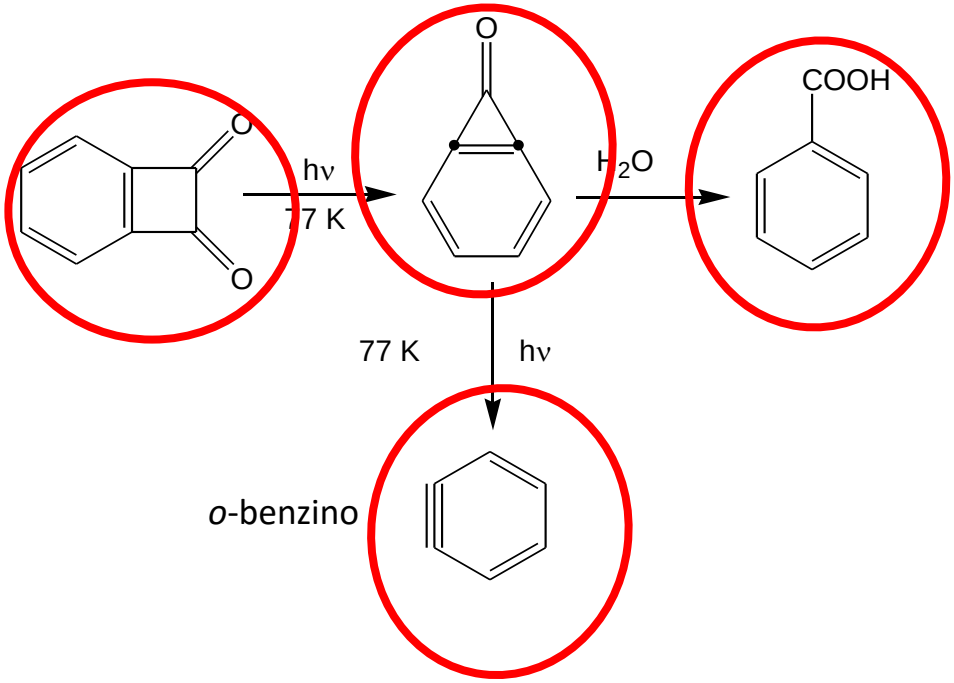

^{1}H e ^{13}C NMR a bassa T

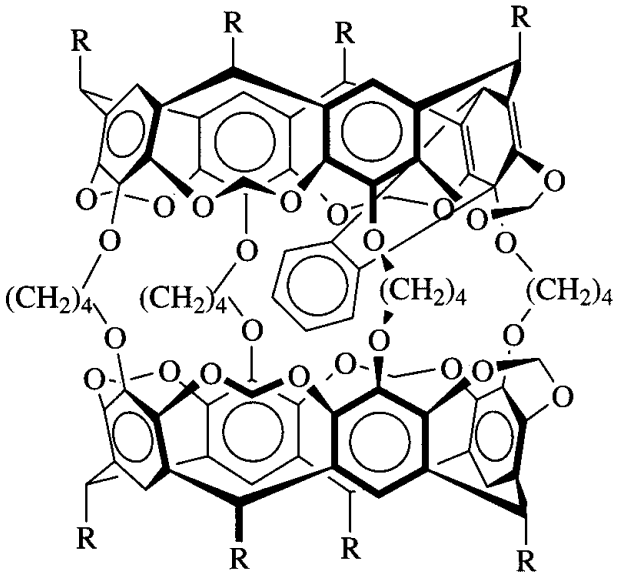

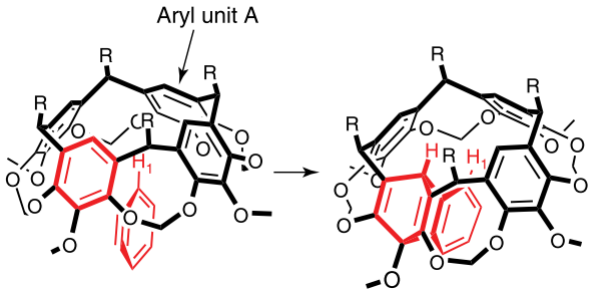

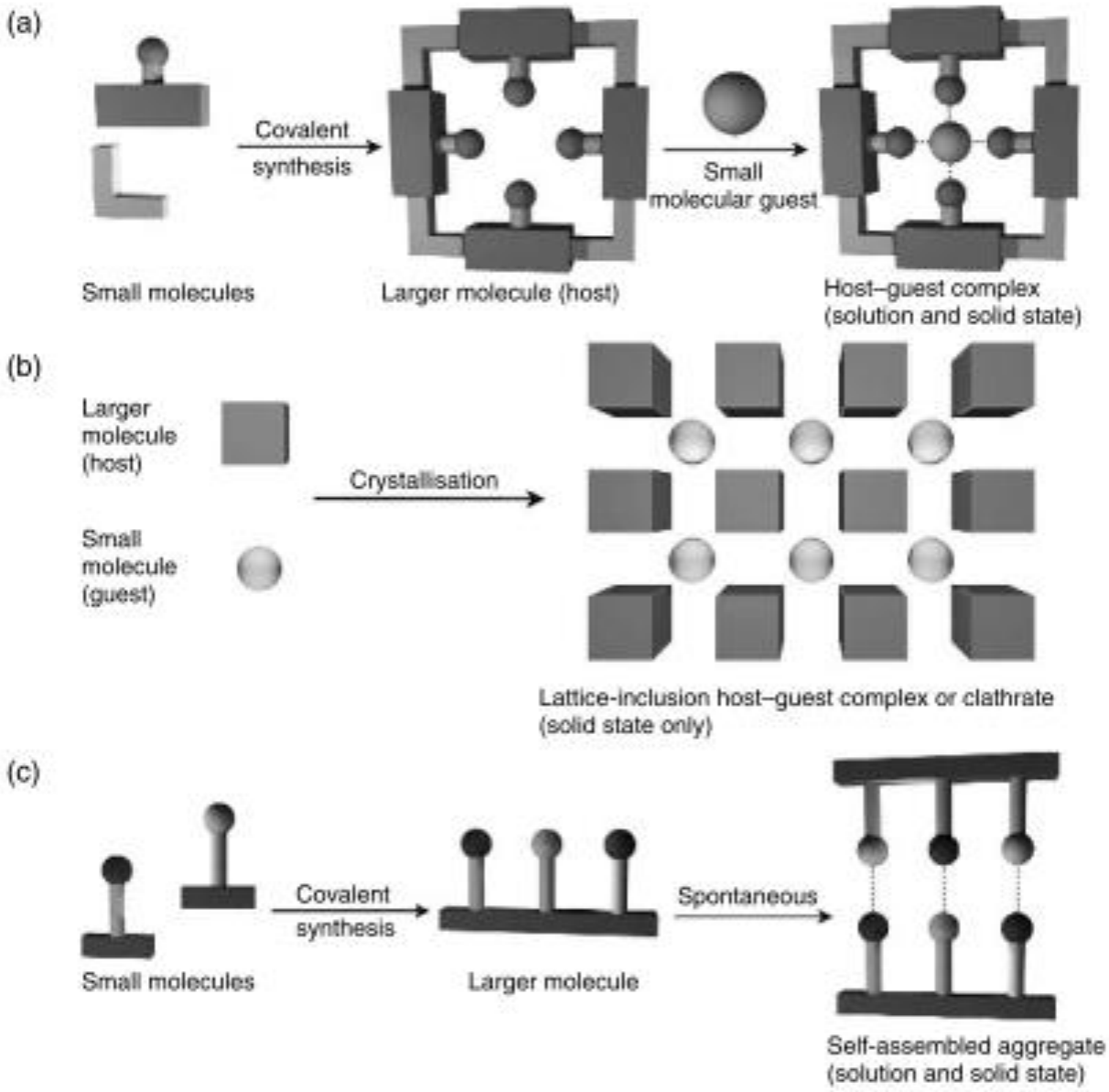
(a)
Covalent
synthesis
Small
molecular guest
Small molecules
Larger molecule (host)
Host–guest complex
(solution and solid state)
(b)
Larger
molecule
(host)
Small
molecule
(guest)
Crystallisation
Lattice-inclusion host–guest complex or clathrate
(solid state only)
(c)
Covalent
synthesis
Spontaneous
Small molecules
Larger molecule
Self-assembled aggregate
(solution and solid state)

Tennis-ball

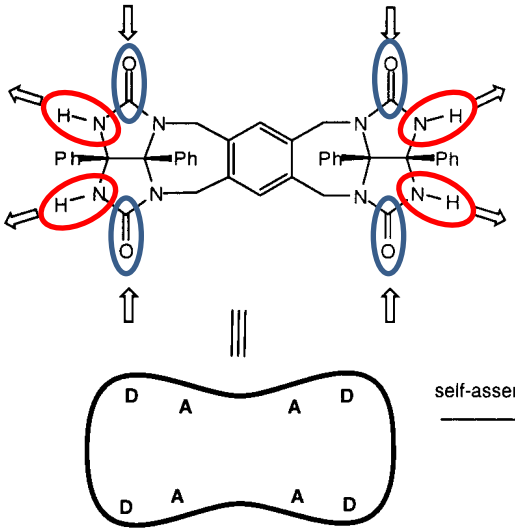

The formation of a molecular tennis ball

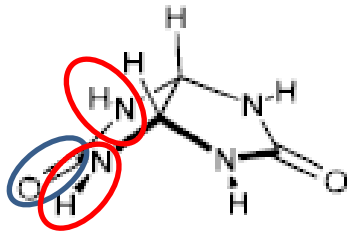

unità glicolurile

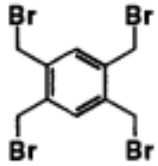

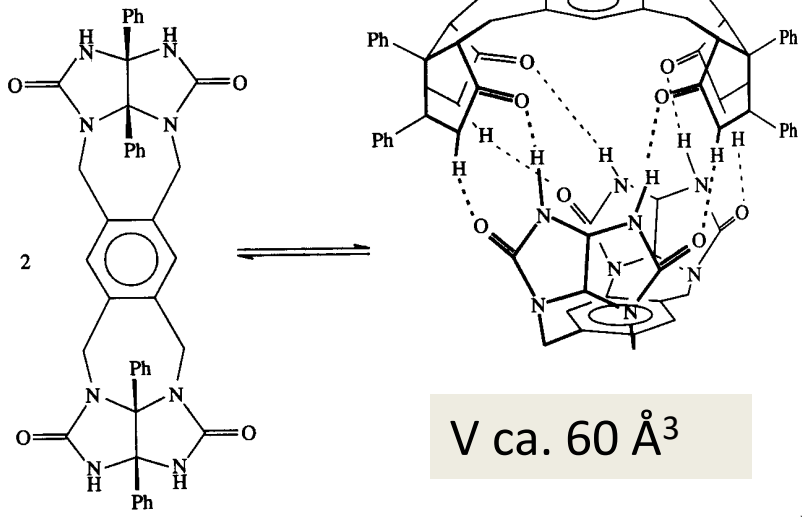

V ca. 60 Å^3

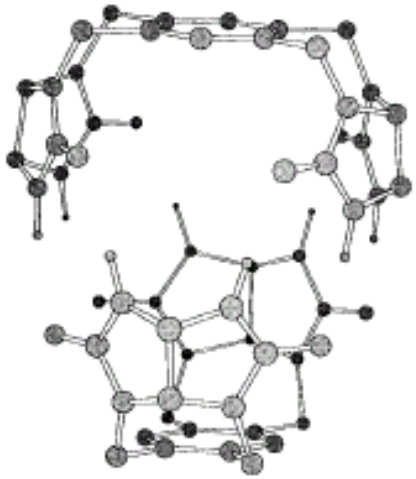

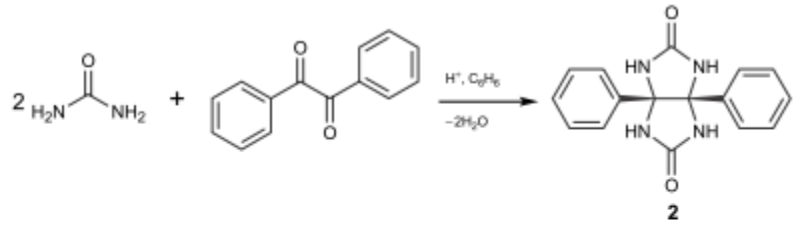
2
H2N
NH2
+
H+, C6H6
−2H2O
HN
NH
O
2

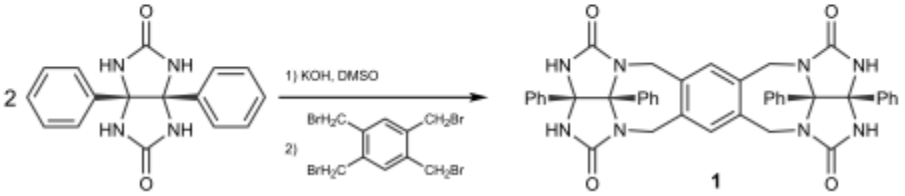
2
1) KOH, DMSO
2)
BrH2C
CH2Br
Ph
1

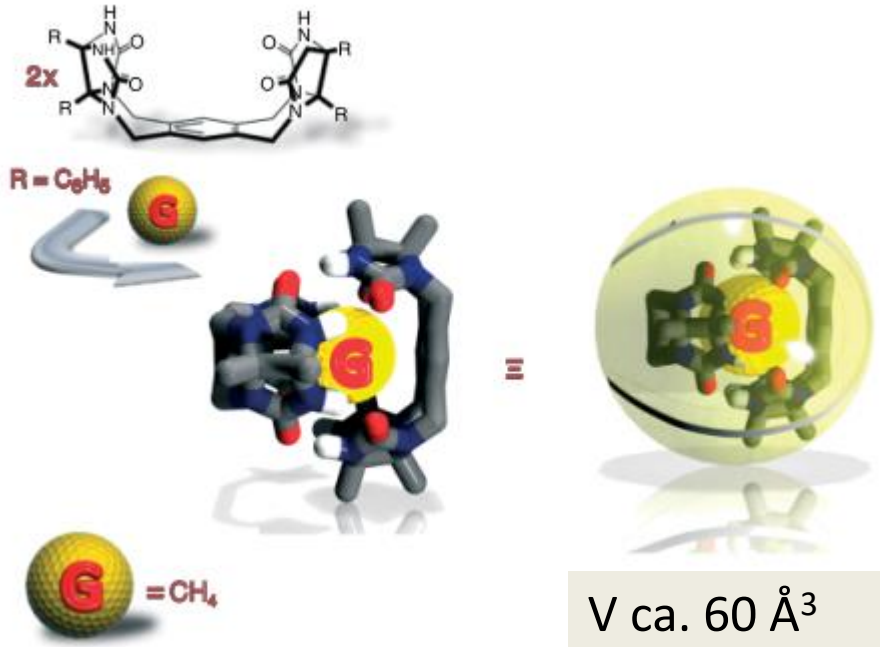
2x
R = C6H5
G
= CH4

V ca. 60 Å^3

Molecular Cylinder

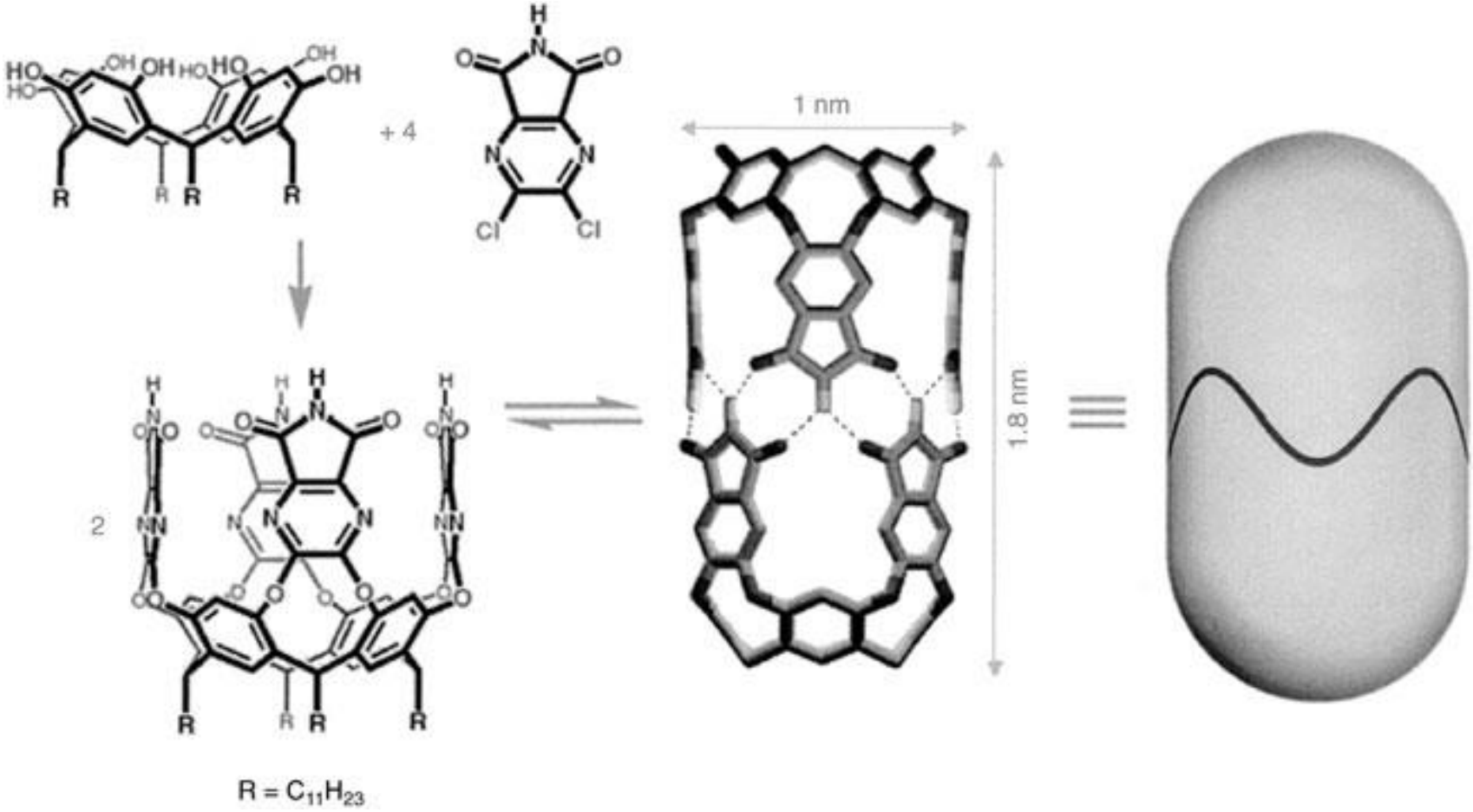

V *ca.* 420 Å^3

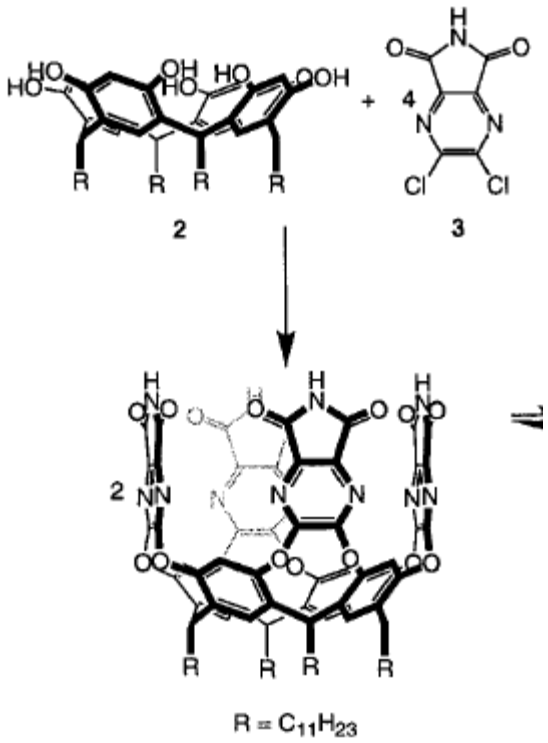

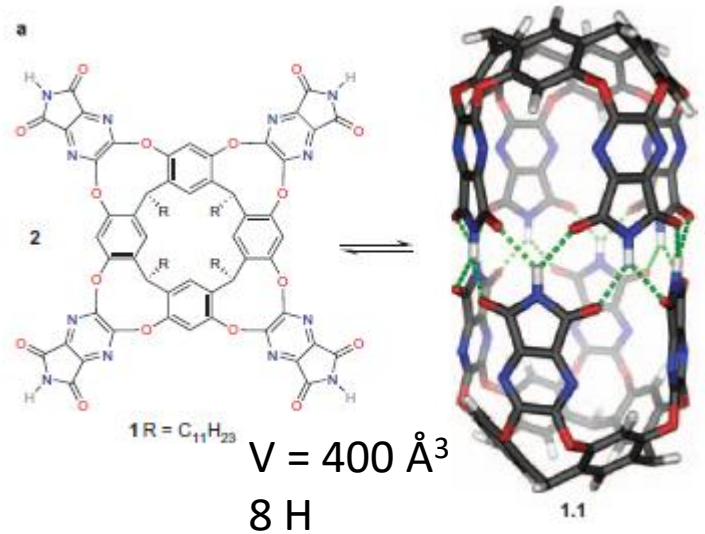

V = 400 Å^3

8 H

16 Å

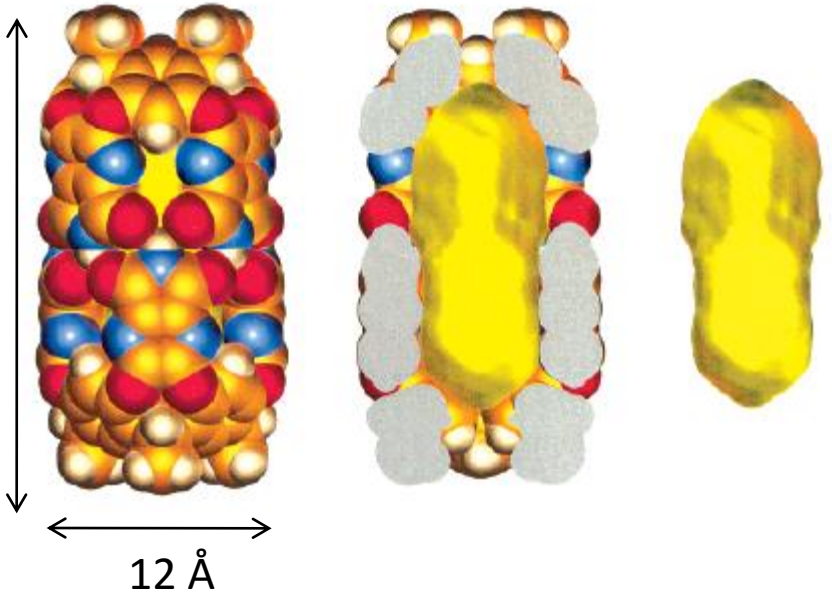

12 Å

From molecular mechanics calculations:

the encapsulated guest(s) occupy approximately 55% of the available space (same occupancy inside most weakly interacting organic solvents).

Stability deacreases at higher or lower space occupancy.

The ins and outs of molecular encapsulation

Liam C. Palmer and Julius Rebek, Jr.*

Org. Biomol. Chem., 2004, **2**, 3051–3059

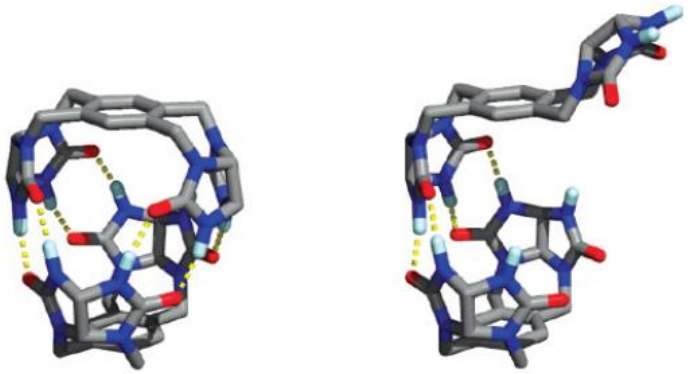

Fig. 5 The intact tennis ball, left, and the conformation with an open flap, right. The structure on the right represents intermediate of a possible "gating" mechanism.

A priori, two plausible exchange mechanisms can be imagined: (1) a dissociative mechanism in which the two capsule subunits completely separate, or (2) a gating mechanism[22] whereby one "flap" of the tennis ball opens by ring inversion of the seven-membered ring (as shown in Fig. 5).

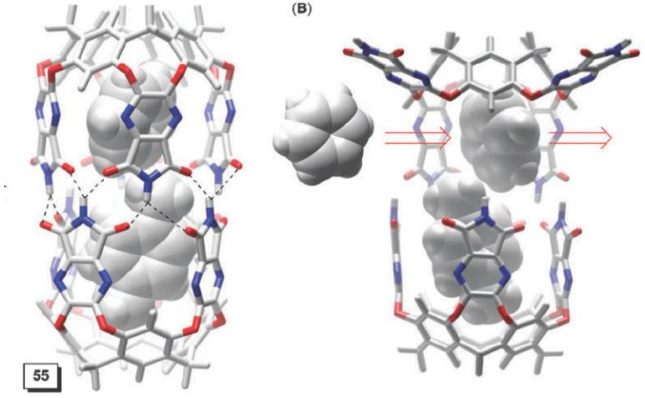

Small guests like toluene can escape by opening of a single flap, left. Larger guests like dimethylbiphenyl require opening of two or more flaps, right.

Contrasting the mechanism in apolar media, the presence of methanol seems to cause large guest exchange by complete dissociation of the capsule subunits. Complexes of small guests are not stable under these conditions.

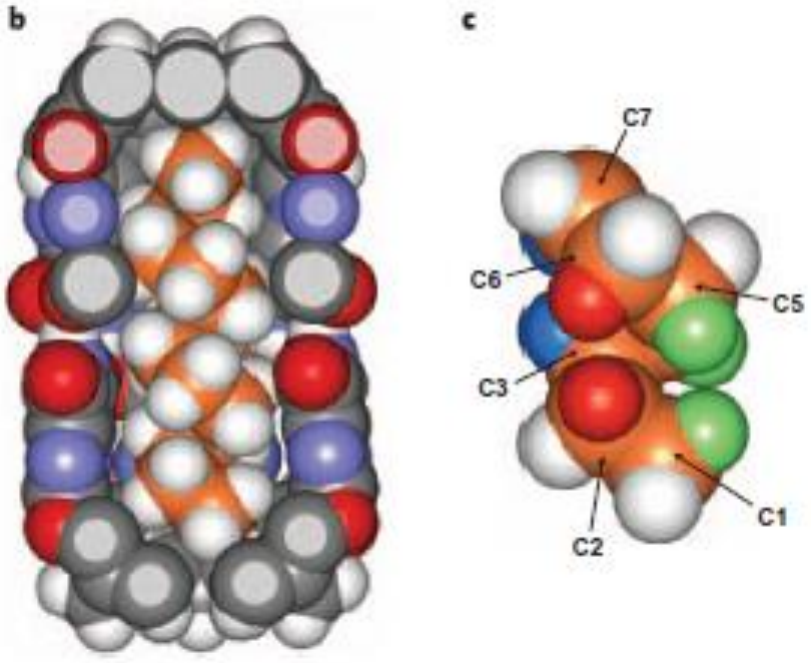

Model structure: incapsulation of coiled alkanes - tetradecane

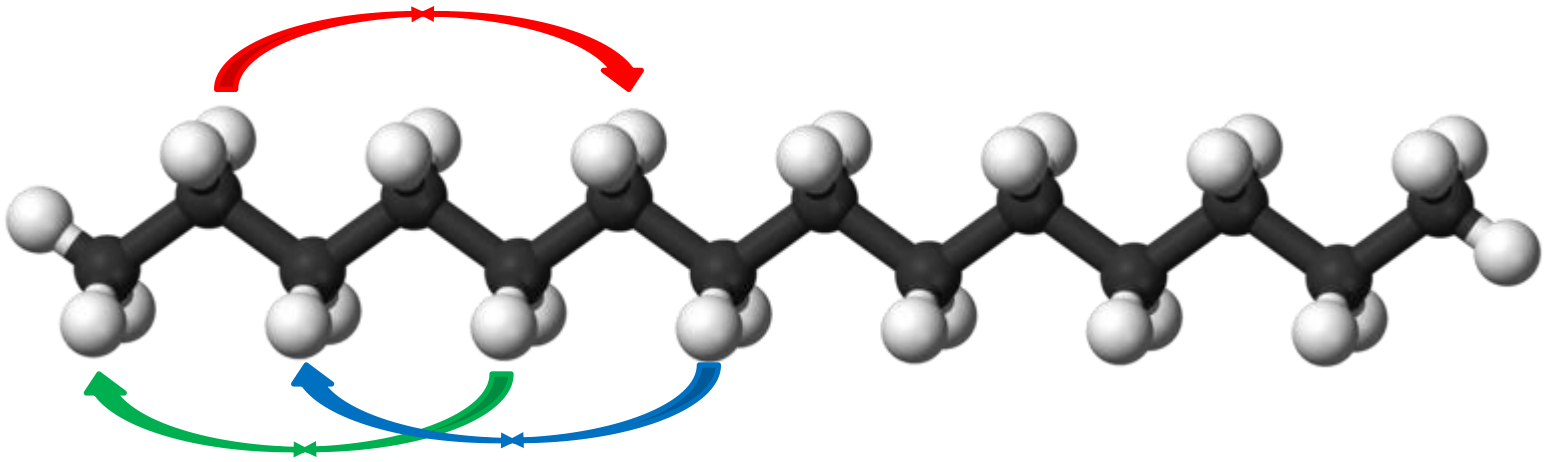

Social Isomers:

A new form of isomerism arises when two different guests are confined to a cylindrical, self-assembled host capsule. The shape and dimensions of the capsule prevent the guests from exchanging positions or tumbling on the NMR time scale. The phenomenon depends on matching guest size and shape with that of the host and on the interaction of the two guest molecules. The orientation of one guest depends on the presence and nature of the other.

Social Isomers

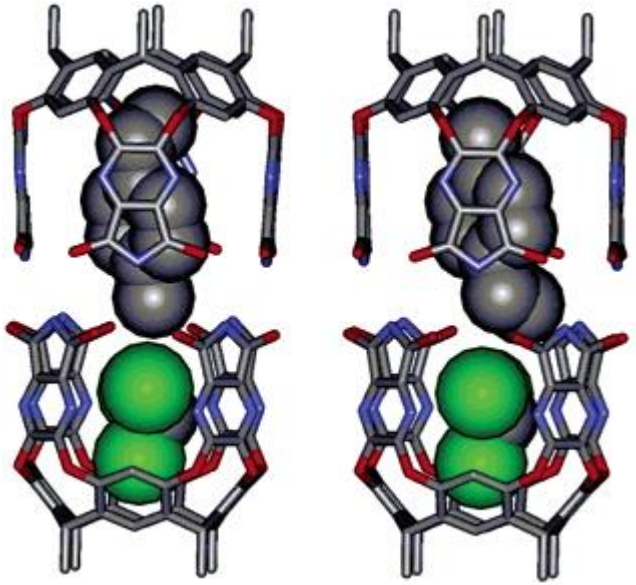

MM optimized structures:
cloroformio e *para*-etiltoluene

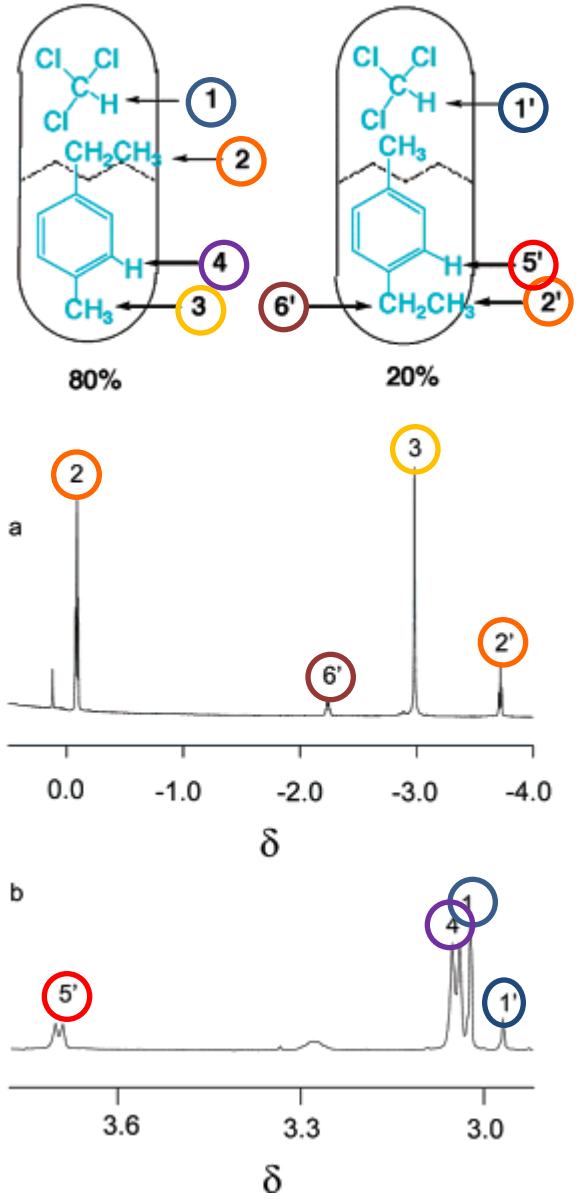

Constellation Isomers

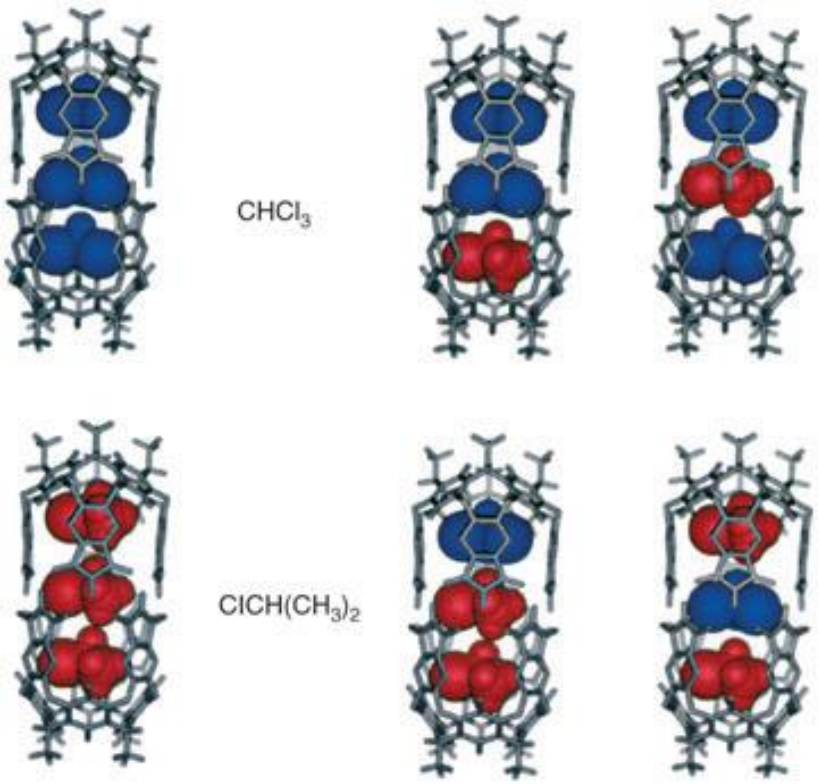

MM optimized structures:
cloroformio e *iso*-propilcloruro

In addition to being able to preserve highly labile species, they may serve as catalysts and accelerate reactions inside their inner cavity by either concentrating the reactants leading to higher effective concentrations or TS stabilization or by preorganising them inside the capsule.

They may create a micro-environment in which two encapsulated reactants are held together in a orientation that differs from their most reactive arrangment in solution (or gas phase) leading to products that are disfavoured in equivalent solution phase reactions.

Reattività nelle capsule molecolari

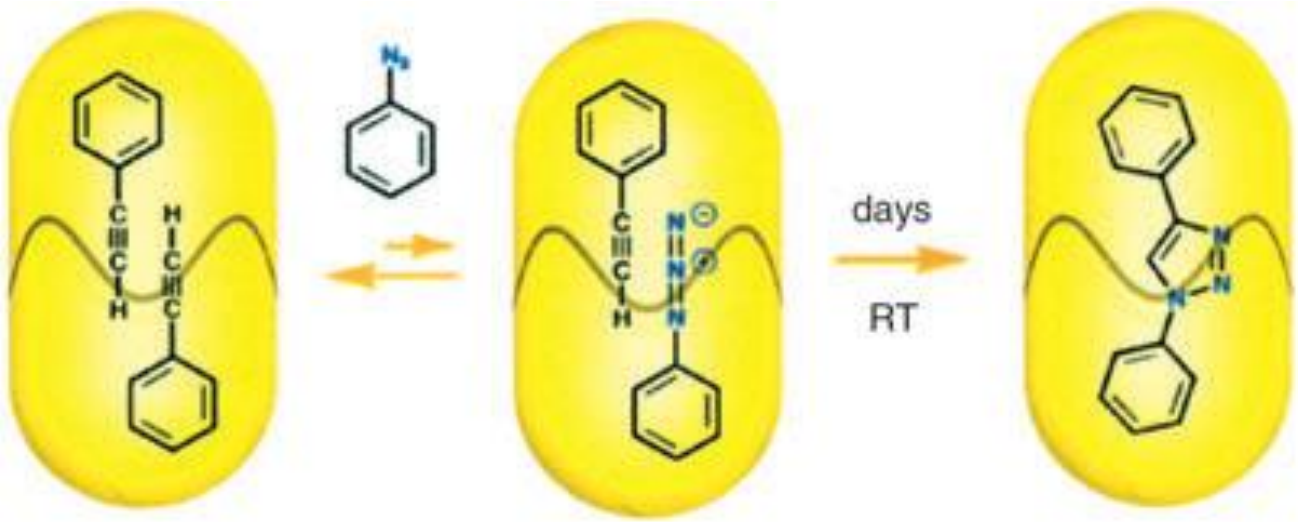

Cicloaddizione 1,3 regioselettiva di fenilacetilene e fenilazide:

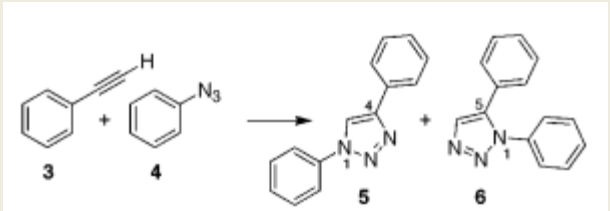

Volume definito = [ ] 4M vs mM
Tempo di contatto = 1 s vs 1 ns
Solvatazione fissa

CB[8] gated photochromism of a diarylethene derivative containing thiazole orange groups†

Yueyuan Mao, Keyin Liu, Guanglei Lv, Ying Wen, Xingjun Zhu, Haichuang Lan and Tao Yi*

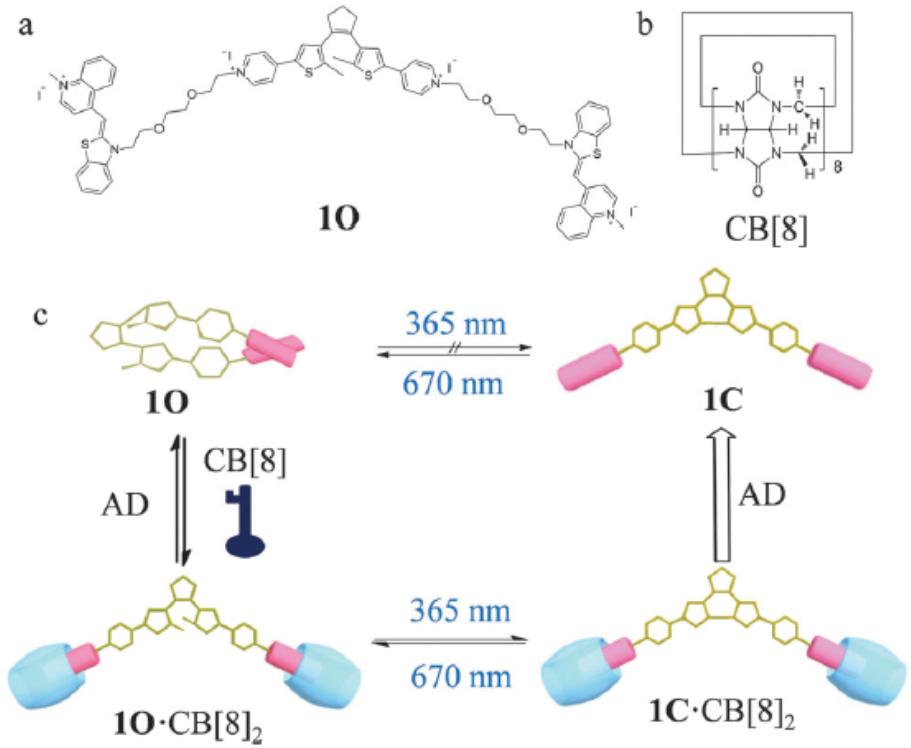

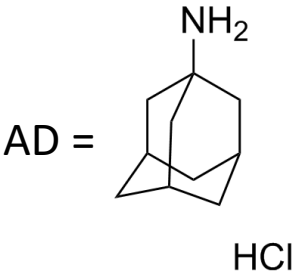

Scheme 1 The chemical structures of (a) **1O** and (b) CB[8]; (c) the schematic diagram for the interaction of **1O** with CB[8] and the photochromic process.

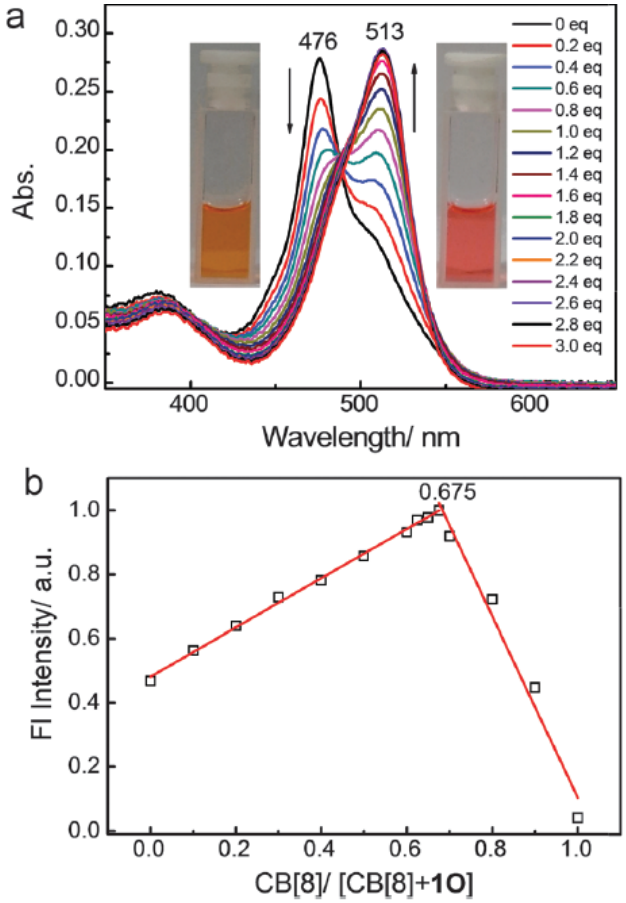

Fig. 2 (a) The UV-visible spectra of **1O** (5 μM) with addition of different equivalents of CB[8]; (b) Job plot of **1O·CB[8]$_2$** for the emission intensity changes at a wavelength of 546 nm with a total concentration of **1O** and CB[8] of 15 μM; square deviations of the fitted lines were 0.99721 and 0.97348, respectively.

1O·CB[8]$_2$ upon addition of different concentrations of **AD**

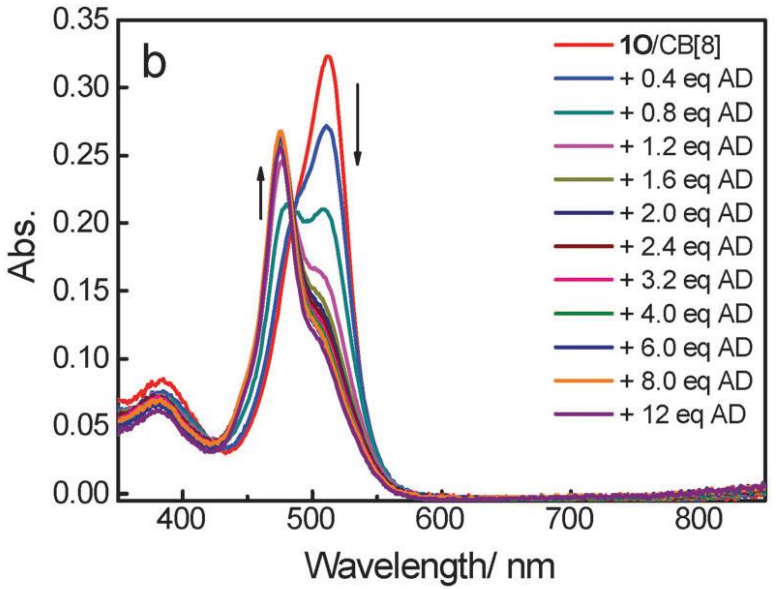

After irradiating the **1O·CB[8]$_2$** complex, the **1C** form was maintained to some extent even after displacement by **AD**: the absorption at 685 nm of the **1C·CB[8]$_2$** generated upon UV light irradiation only decreased by 50%. This indicated that **1C·CB[8]$_2$** was dissociated into **1C** but only half of the closed ring isomer converted to its open form (**1O**). The **1C** generated in this way was stable for at least 5 hours and could be converted to the open form again upon irradiation with 670 nm laser light.

Host–Guest Chemistry

Angew. Chem. Int. Ed. 2010, 49, 3192 –3195

Photochemical Control of Reversible Encapsulation

*Henry Dube, Dariush Ajami, and Julius Rebek, Jr.**

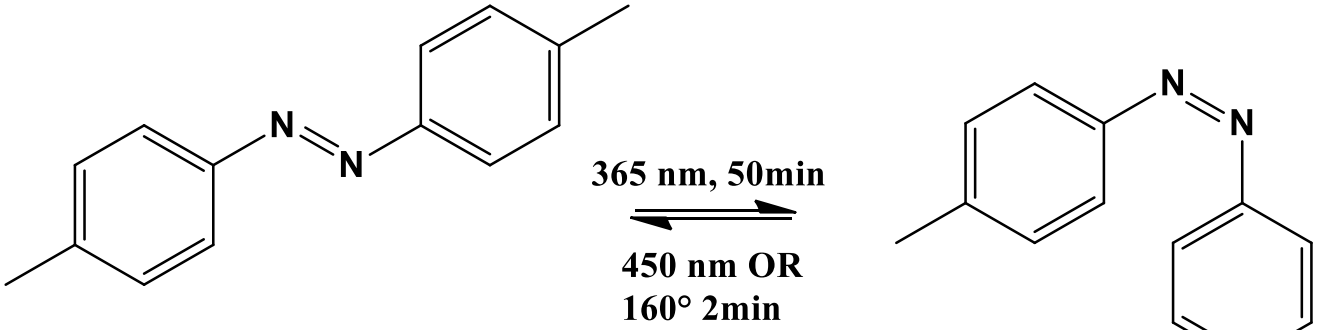

trans-4,4'-dimethylazobenzene (*trans*-**1**) (*cis*-**1**)

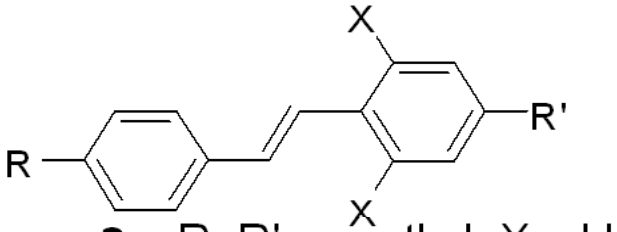

R, R' = methyl, X = H

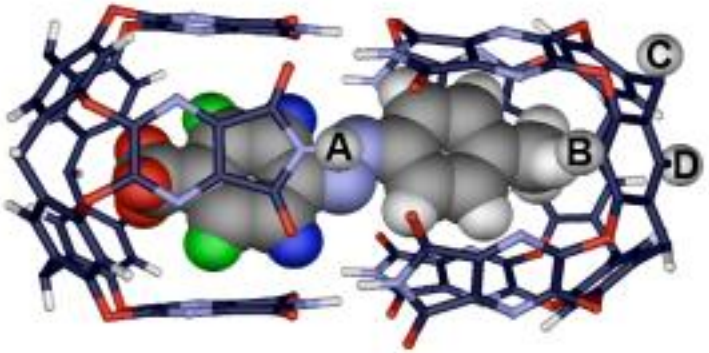

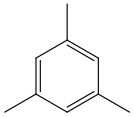

[D_{12}]mesitylene

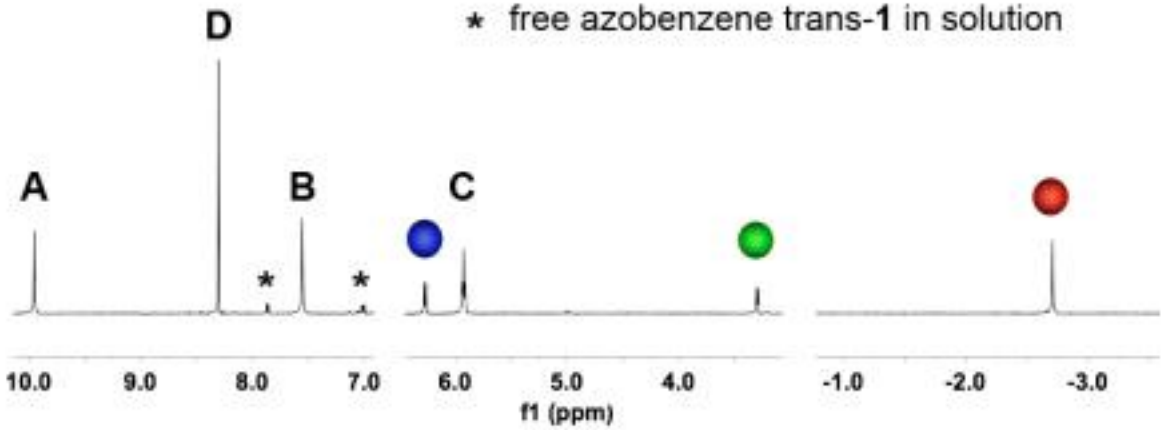

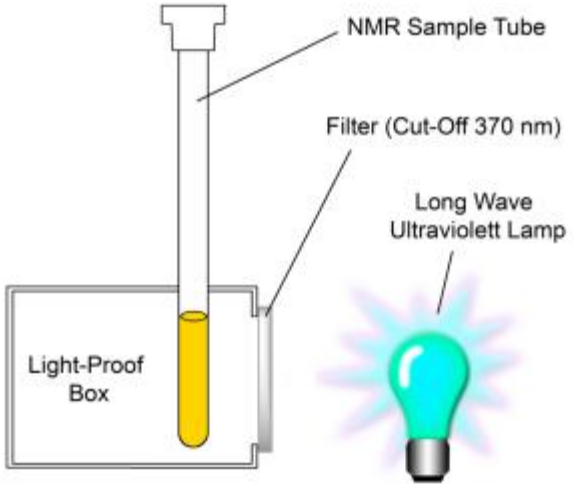
NMR Sample Tube
Filter (Cut-Off 370 nm)
Long Wave
Ultraviolett Lamp
Light-Proof
Box

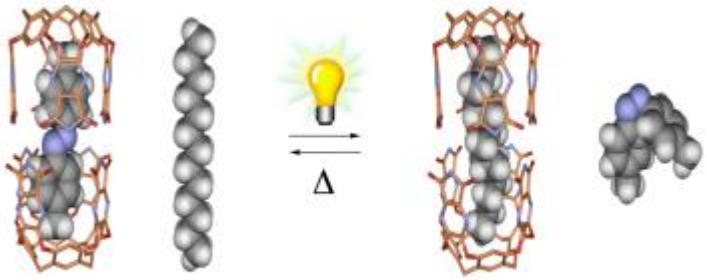
Δ

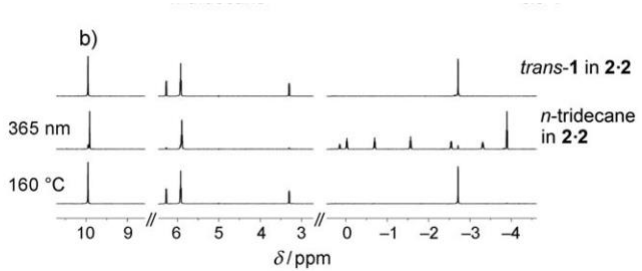
b)
trans-1 in 2·2
365 nm
n-tridecane
in 2·2
160 °C
10 9 6 5 4 3 0 −1 −2 −3 −4
δ / ppm

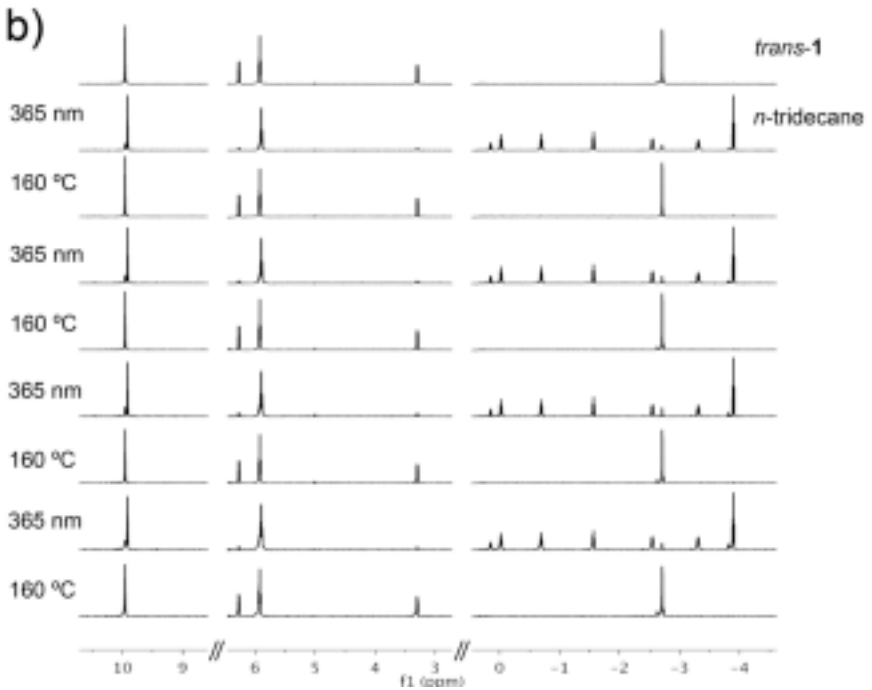
b)
trans-1
365 nm
n-tridecane
160 °C
365 nm
160 °C
365 nm
160 °C
365 nm
160 °C
10 9 6 5 4 3 0 -1 -2 -3 -4
f1 (ppm)

Guest =

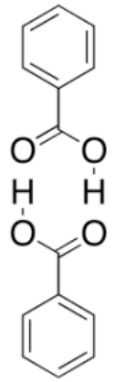

Guest =

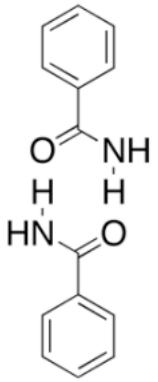

a)

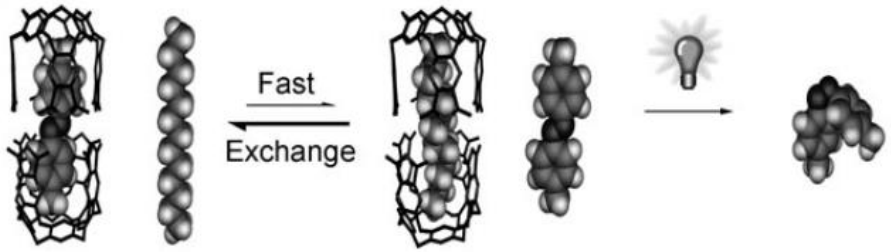

b)

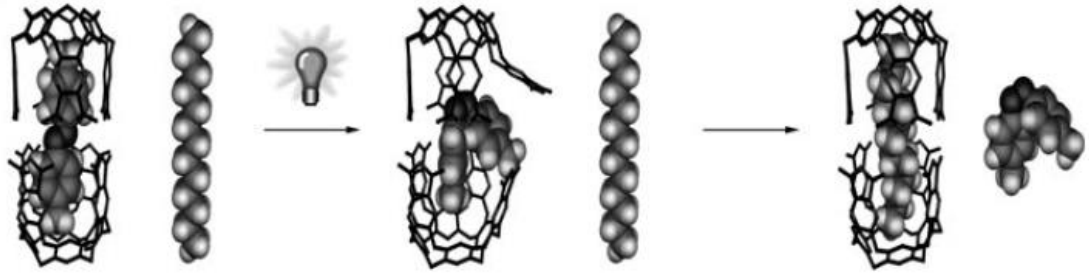

Breakout

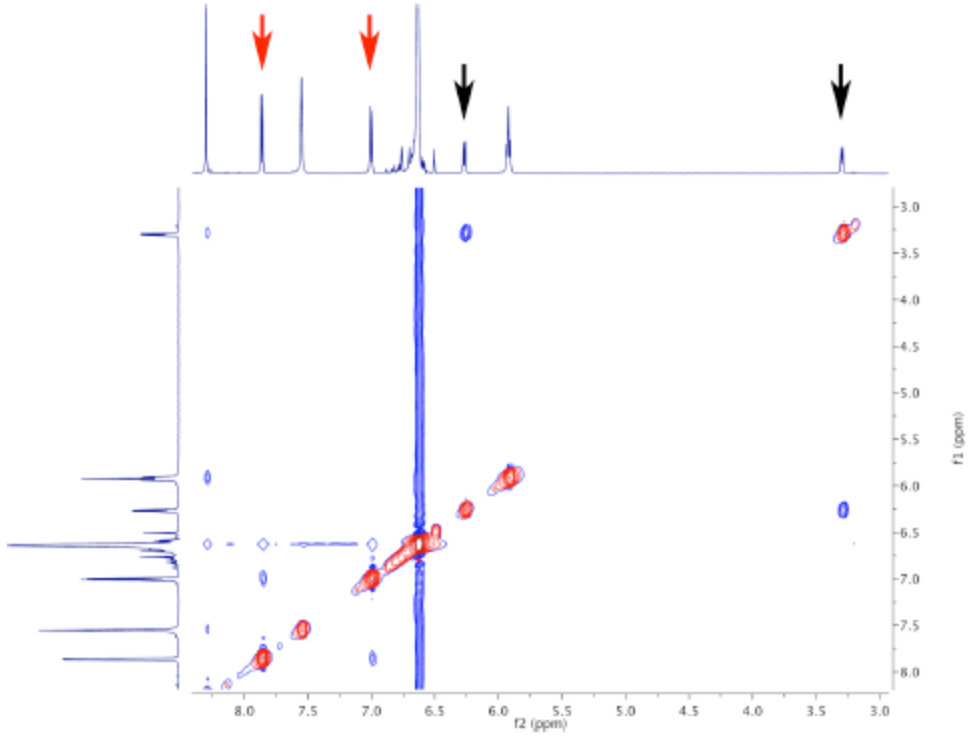

Figure 6SI: Partial ^{1}H NMR ROESY spectrum (mesitylene-d_{12}, 300 K, mixing time = 0.3 s, D1 = 1.5 s) of the host guest complex of *trans*-**1** and **2**•**2** in the presence of 1.5 equiv. *trans*-**1** free in solution. Red arrows assign the aromatic signals of free *trans*-**1** whereas black arrows assign the aromatic signals of encapsulated *trans*-**1**. No exchange signals between these signals can be observed as the guest exchange is slow.

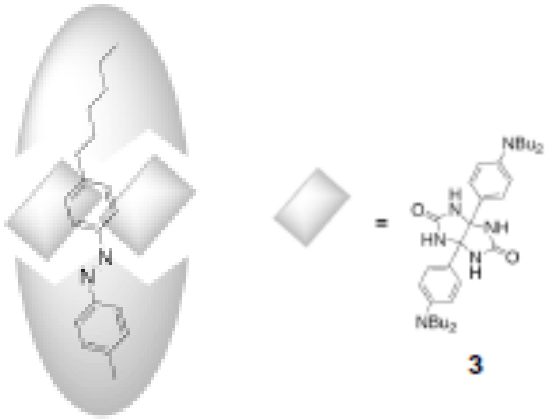

NBu2
NBu2

3

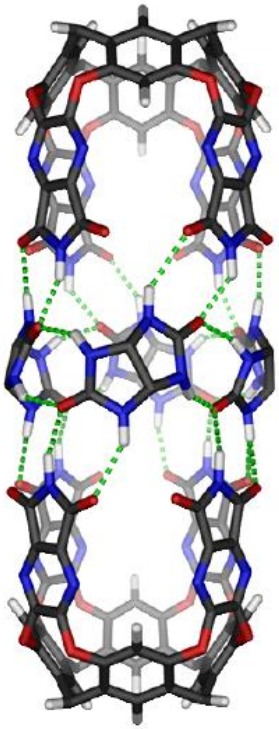

≡

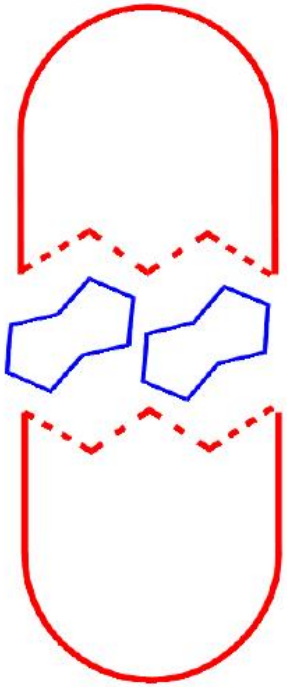

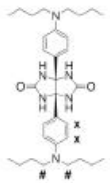

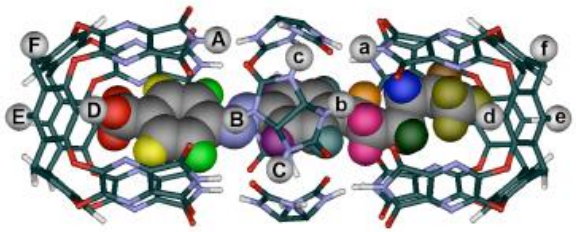
F
A
c
a
f
E
D
B
b
d
e
C

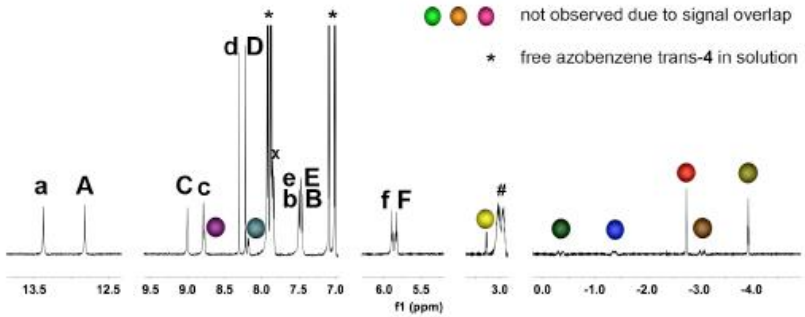
not observed due to signal overlap
free azobenzene trans-4 in solution
a A
C c
d D
e E
b B
f F
#
13.5
12.5
9.5
9.0
8.5
8.0
7.5
7.0
6.0
5.5
3.0
0.0
-1.0
-2.0
-3.0
-4.0
f1 (ppm)

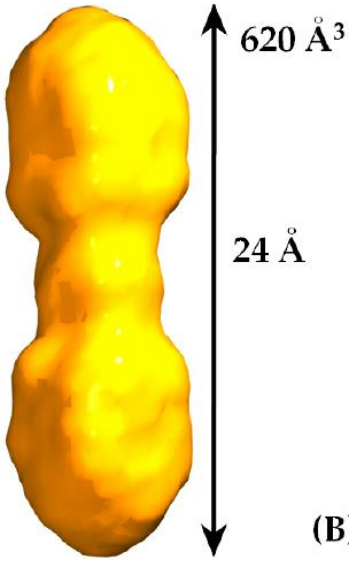
620 Å3
24 Å

(B

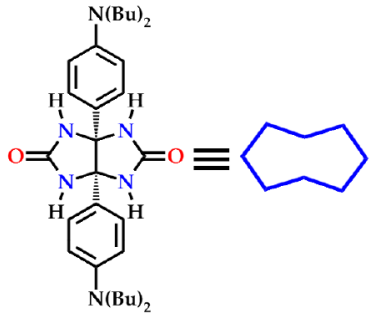
N(Bu)2
N(Bu)2

≡

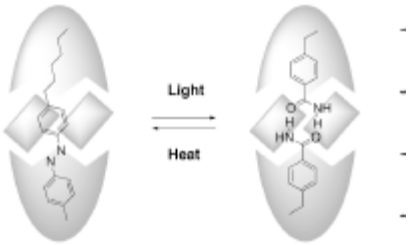
Light
Heat

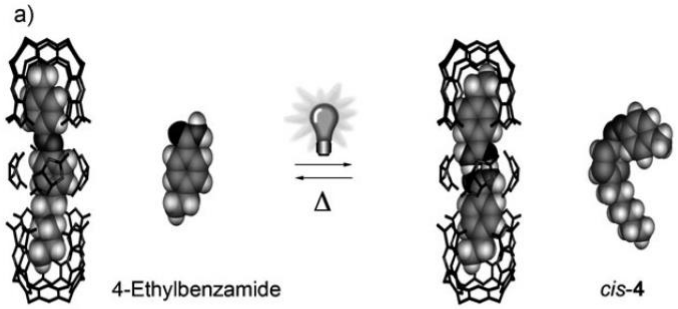
a)
Δ
4-Ethylbenzamide
cis-4

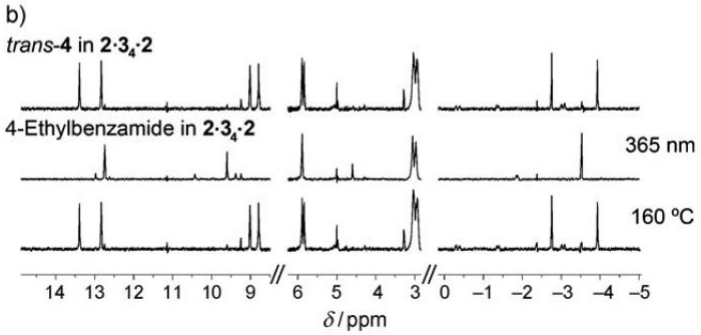
b)
trans-4 in 2·3₄·2
4-Ethylbenzamide in 2·3₄·2
365 nm
160 °C
14 13 12 11 10 9 6 5 4 3 0 –1 –2 –3 –4 –5
δ / ppm

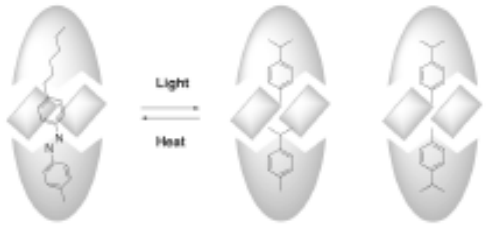
Light
Heat

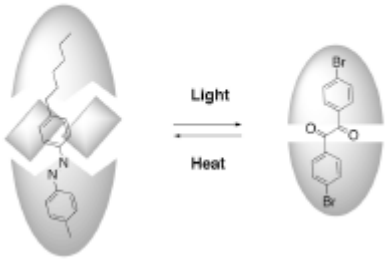

a)

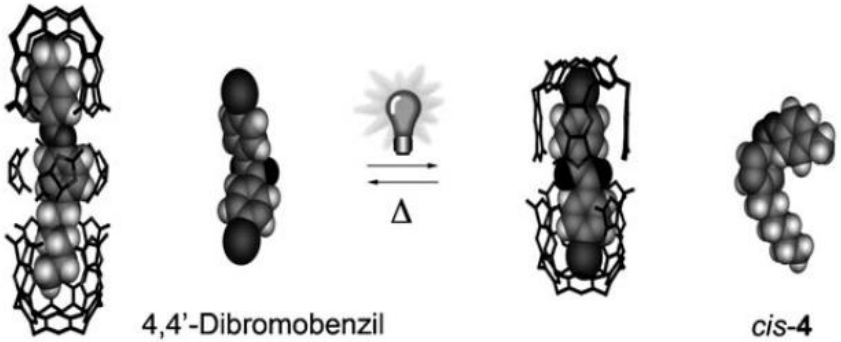

4,4'-Dibromobenzil

cis-**4**

b)

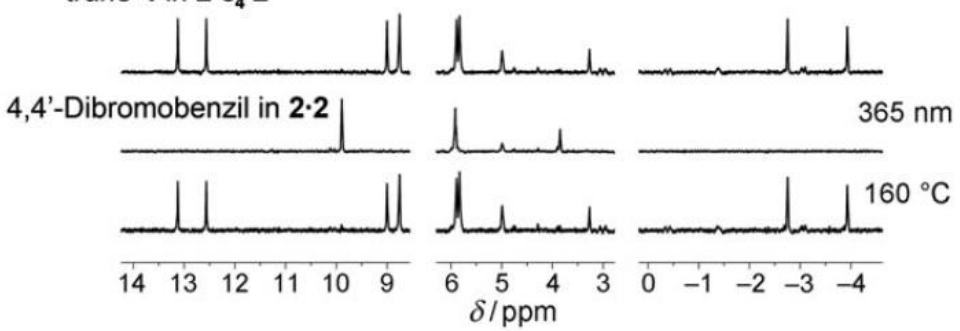

Soft Ball

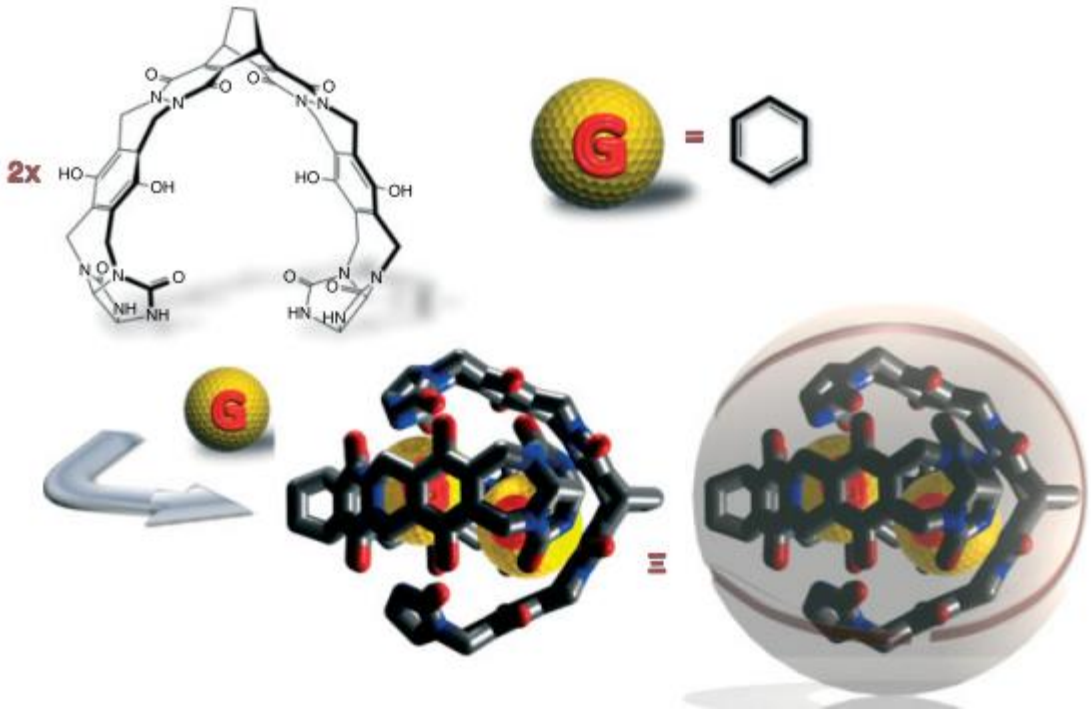

V ca. 400 Å^3

Reattività nelle capsule molecolari

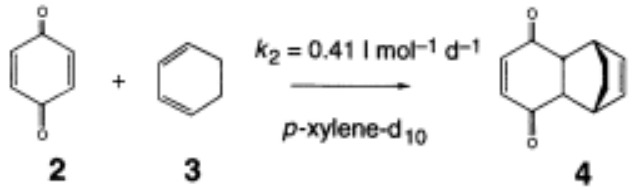

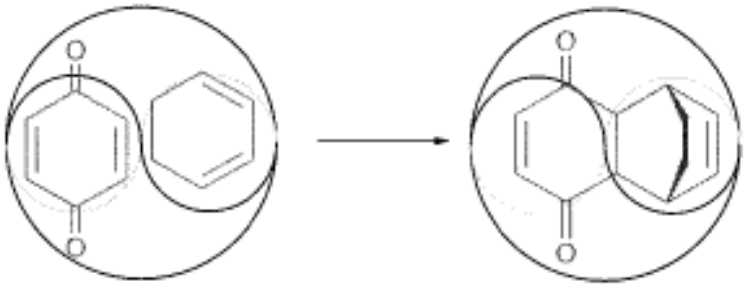

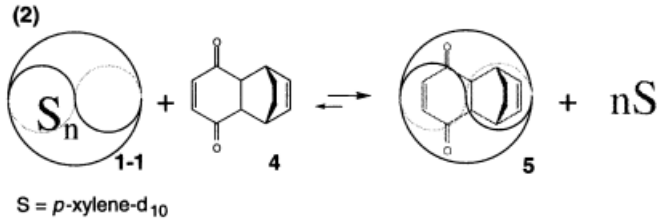

Reattività nelle capsule molecolari

Cicloaddizione Diels-Alder acceleraz di ca. 200 volte
[ ] = 5M
Solvatazione
Tempo di contatto